RESWITCHING TRANSIENTS IN INDUCTION MOTOR DRIVES

A DISSERTATION

submitted in partial fulfilment of the requirements for the award of the degree of

MASTER OF ENGINEERING

in

ELECTRICAL ENGINEERING

(Power Apparatus and Electric Drives)

CKED
1995

177801
21-5-84

By

NAVIN S. CHITORE

DEPARTMENT OF ELECTRICAL ENGINEERING
UNIVERSITY OF ROORKEE
ROORKEE-247667 (INDIA)

July, 1982

C E R T I F I C A T E

Certified that the thesis entitled 'RESWITCHING TRANSIENTS IN INDUCTION MOTOR DRIVES' which is being submitted by Shri N.S.Chitore for the award of the degree of Master of Engineering in Electrical Engineering (Power Apparatus and Electric Drives) of University of Roorkee, is a record of student's own work carried out by him under my supervision and guidance. The matter embodied in this thesis has not been submitted for the award of any other degree or diploma.

This is further to certify that he has worked for a period of 7 months from January 1982 to July 1982, for preparing this thesis for Master of Engineering degree at this University.

S. P. Gupta

(S.P.GUPTA)
Lecturer
Electrical Engg. Department
University of Roorkee
Roorkee (U.P.)

ROORKEE :

DATED: JULY 21 ,1982.

DEDICATED TO MY

MOTHER

A CONSTANT SOURCE OF INSPIRATION

A C K N O W L E D G E M E N T S

The author acknowledges his deep gratitude to Shri S.P. Gupta, Lecturer in Electrical Engineering Department, University of Roorkee, for his unfailing inspiration and valuable guidance given by him during the course of this work.

Sincere thanks are due to Dr. D.R. Konli, Head of Electrical Engineering Department, University of Roorkee, for providing various facilities in connection with this work.

The author also wishes to thank staff of Computer Centre and P.G. Laboratory for their help during this work.

Finally the author is grateful to his friends who have contributed directly or indirectly to the success of this work.

ROORKEE

NAVIN S. CHITORE

DATED : JULY ,1982

A B S T R A C T

Predicting transient performance of induction motor, for given bus-transfer conditions, is one of the important problems faced by system designers. Looking to the literature published so far, it is noted that, most of the authors have considered speed of the motor during supply change-over interval, as constant. The work presented in this thesis gives in detail the calculation of reswitching(reclosing) transients in induction motor drives, by considering speed as one of the variables. The drive considered here is a slip ring induction motor whose slip power is wasted in externally connected resistance for the purpose of speed control. The variation of resistance is achieved by a chopper circuit connected in the rotor circuit.

Induction motors, by and large, operate on uninterrupted power supply. Large induction motors, using high voltage supply with direct-on-line switching, however, face momentary interruptions of power supply due to two reasons -

i) Fault in the supply system which takes about 10 cycles to clear.

ii) Emergency bus transfer.

During this small period of interruption the motor terminals are open and a voltage appears across them which keeps on changing its phase and magnitude with time. This

voltage is known as open-circuit or residual or motor-self-generated voltage. If the power supply is restored to motor at an instant when bus voltage and the residual voltage are out of phase by 180^{o} and residual voltage is substantial in magnitude, the effective voltage would be very high and will produce excessive forces. This may damage the motor in following manner -

i) Stator coils may become loose in the slots

ii) The shaft may twist

iii) The motor may even be ripped from its base plate

In this work, the transient results have been thoroughly examined to evolve the safe time for reclosure which may be used to design the protective scheme of the motor to save it from this hazard.

The mathematical model for analyzing the steady state and transient behaviour of chopper controlled slip ring induction motor has been developed using synchronously rotating reference frame. The parameters involved in these equations are such that they can be easily measured experimentally at the terminals of the induction machine. Here the effect of saturation has not been taken into account.

In order to investigate the transient behaviour, the non-linear differential equations describing the dynamics of the system have been simulated on a digital computer and solved by the application of Runge-Kutta method. As the most

important transients from electromechanical considerations are those of electromagnetic torques and speed, these are investigated in detail. The effects of system inertia and of applied voltage are also studied on torque transients. Experimental results are also included.

This work will, thus, be found useful in two ways -

i) It presents a general approach of formulating mathematical model for induction motor, which is useful in predicting the safe reclosure time for large machines.

ii) The chopper controlled slip ring induction motor drive has been studied and the results of reclosing transients provided.

TABLE OF CONTENTS

LIST OF SYMBOLS

v	=	instantaneous value of voltage
i	=	instantaneous value of current
V_1	=	rms value of stator phase voltage
V_2	=	rms value of rotor phase voltage
R_1, R_2	=	stator and rotor resistance, per phase
L_{11}, X_{11}	=	self inductance and reactance, respectively of stator
L_{22}, X_{22}	=	self inductance and rectance, respectively of rotor
L_{12}	=	mutual inductance between stator and rotor
s	=	per unit slip
p	=	differential operator, d/dt
P	=	number of poles on motor
E_A	=	open circuit voltage
T_E, T_L	=	developed torque and load torque of motor
H	=	motor inertia constant, sec.
X_m	=	mutual reactance referred to stator
F_R	=	frequency ratio
w	=	electrical angular speed in rad/sec.
w_r	=	mechanical angular speed in p.u.
ϱ_o	=	any arbitrary phase angle between stator and rotor phases.
T_1	=	number of turns per phase of stator winding
T_2	=	number of turns per phase of rotor winding

a	=	stator/rotor turns ratio (T_1/T_2)
I_{DC}	=	average dc current supplied by rectifier
R_{ex1}, R_{ex2}	=	External resistance referred to stator
δ	=	duty cycle of chopper
T_{VRM}	=	Time at which maximum resultant voltage occurs.
T_{WR}	=	Worst reclosure time
WPTE	=	Worst peak torque
V_S	=	Supply voltage
T_o	=	Open circuit time

Subscripts

a,b,c	=	phase quantities
d,q	=	direct and quadrature axis quantities
s,r	=	stator and rotor quantities respectively.

CHAPTER-I

INTRODUCTION

With the progress in automation, there is a growing demand for precise and reliable variable-speed drives which have the ability to respond quickly and accurately to external speed and torque demands. The adjustable speed ac motor drives are popular as the ac motor is cheap, simple in construction and more economical to operate and maintain. In the majority of cases, an induction motor will be used because of its low capital cost, simple construction and absence of commutator problems.

As a result of recent advances in solid state technology and with the availability of reliable and efficient thyristors in high power ratings, the use of schemes which employ stator voltage control, frequency control, rotor resistance control are becoming more popular. Though the schemes employing stator voltage control and frequency control seem to be very attractive, because they enable a squirrel cage induction motor to be used which is robust, rugged and cheap, they have a number of disadvantages associated with them. The limitations of stator voltage control are the limited sub-synchronous speed range, unsuitability for constant torque operation and the problem of thyristor turn off at low speeds because of low energy storage in commutating capacitors. In frequency changing schemes commutation and triggering logics

are very complex making the inverter more sophisticated and hence the scheme becomes uneconomical for small and medium size drives. Moreover this system exhibits a large region of instability at low values of frequencies, thus making the system unsuitable for low speeds. The variation of speed by rotor resistance control is very simple and reliable, but it is very inefficient, because of wastage of power in the additional rotor resistances. Still this method holds feasibility where deviation from normal operating speed is needed for small intervals. It provides high starting torque with low starting current and variation of speed over a wide range below the synchronous speed of the motor. Smoothness of speed control depends upon the number of steps of resistance that are available. This type of control is used when the load is of an intermittent nature, requiring high starting torque and relatively rapid acceleration and retardation, such as foundry or steel mill hoists and cranes. The rotor resistance is altered manually and in discrete steps. This mechanical operation is undesirable because the time response is slow and speed variation is not smooth. With the recent progress in power semiconductor technology, these undesirable features of the conventional rheostatic control scheme can be eliminated by using a three-phase rectifier bridge and a chopper-controlled external resistance. The chopper electronically alters the external resistance in a continuous and a contactless manner.

N.S. Wani and M. Ramamoorty[34] have investigated a thyristor controlled chopper circuit for the speed control of slipring induction motor drive. A thorough analysis of the steady state performance of the system is provided for the following cases -

i) Without filter on the rotor side.

ii) With Ist order filter on the rotor side

iii) With 2nd order filter on the rotor side.

Experimental results are given for open loop and closed loop control scheme with speed and current feedback.

P.C. Sen and K.H.J Ma[32] have also used a solid state speed regulating scheme for induction motor using a rotor chopper-controlled external resistor. A thorough analysis of the steady-state performance of the system is presented. Both dc and ac circuit models are derived to describe the performance characteristics when the chopper operates under the time ratio control strategy. Effects of machine parameters on performance characteristics are studied. Theoretical results from the model are verified by comparison with experimental results.

M. Ramamoorthy, E. Waltman and N.S. Wani[33] have again investigated the thyristor controlled chopper circuit used for the speed control of slip ring induction motor. They come to conclusion that simple chopper circuit (i.e. one without additional inductance in series) produces

discontinuous rotor currents and causes excessive rotor heating. The speed range obtainable by the simple chopper is also limited.

CONTRIBUTION BY AUTHOR

A mathematical model has been developed for analyzing the steady state and transient behaviour of system. In order to derive the above, the system is analyzed in a synchronously rotating reference frame. The developed model involves such parameters which can be measured experimentally at the terminals of the induction motor.

Steady state equations of the system have been derived from d-q model. The performance characteristics under steady state conditions have been computed from these steady state equations. In case of plain induction motor (i.e. induction motor without any external resistance), a good correlation is obtained between experimental and computed results.

The non-linear first order differential equations describing the dynamics of the system have been simulated on a digital computer and solved by the application of Runge-Kutta method to study the transient behaviour of the system. Switching transients of electromagnetic torque and speed have been investigated when the drive is started from rest under

different loading conditions. The transient behaviour has also been studied when the drive is reconnected to the supply after brief interruption of supply. The effect of system inertia and applied voltage, on the torque and speed transients have been investigated.

Experimental oscillograms have also been given under different transient conditions.

CHAPTER - II

SYSTEM EQUATIONS

The performance of the chopper controlled slip ring induction motor, under transient as well as steady state conditions, can be represented by a set of system equations. These system equations for the chopper controlled slip ring induction motor have been developed in this chapter, using the concept of direct and quadrature axis components, initially proposed by Park, and extended by various authors. The system has been analyzed in a synchronously rotating reference frame. Expressions for the average value of static converter variables are also written down. The equations of the overall system are established from the equation of induction machine and from the equations which express the average values of the converter variables. The circuit equations have been so simplified that the electrical characteristics can be represented by a set of four simultaneous differential equations of the first order. An equation of the electromagnetic torque completes the set of system equations used in the study.

2.1 INTRODUCTION

Fig. 2.1 gives a schematic diagram of chopper controlled slip ring induction motor. In this scheme, the rotor winding of the induction motor is connected to the three phase full wave diode bridge. DC terminals of 3-phase uncontrolled bridge are connected to external resistance - chopper combination.

A chopper is a power switch electronically monitored by a control circuit. When the chopper is in the ON mode all the time, the equivalent external resistance in the rotor circuit is parallel combination of REX_1 and REX_2. When the chopper is in the OFF mode all the time, the external resistance in the rotor circuit is REX_1. If the chopper is periodically regulated so that, in each chopper period, it is ON for some time and OFF for the rest, it is possible to obtain variation of equivalent resistance between REX_1 and $\frac{REX_1 \times REX_2}{REX_1 + REX_2}$. The chopper electronically alters the external resistance in a continuous and contactless manner. Also the rectified current builds up during the ON time interval but decays during the OFF time interval.

Representation of the chopper controlled slip ring induction motor by the circuit equations derived in this chapter is based on the assumption of an ideal machine. This assumption, commonly employed in representing a machine by circuit equations, implies the following.

i) Magnetic saturation is neglected.

ii) Hysteresis and eddy current effects are not taken into account.

iii) Voltage drop in rectifier is neglected.

2.2 DEVELOPMENT OF MATHEMATICAL MODEL FOR THE SYSTEM

The overall system comprises of a 3-phase slip-ring induction motor, uncontrolled rectifier bridge and a

chopper with external resistors. Hence the performance equations of the overall system can be obtained from the equations of symmetrical induction machine and from the equations which express the average values of uncontrolled rectifier bridge.

The generalised equations describing the behaviour of induction machine under transient and steady state conditions are established by considering it as an elementary two pole idealised machine. The effect of number of poles is taken into account by multiplying the expression for torque by the number of pole pairs.

A schematic diagram of an ideal 3-phase induction motor is shown in Fig.2.2(a), wherein it is regarded as a group of linear coupled circuits. Distributed stator and rotor windings have been shown by concentrated coils. The magnetic axes of the individual stator and rotor phases have also been marked in Fig.2.2(a). The connections and current conventions for the stator and rotor phases are shown in Fig.2.2(b).

2.2.1. Equations for Induction Motor

It is more convenient to approach the problem from the concept of generalized tneory of machines. In this approach, the circuit model and its mathematical formulation are obtained through a set of simple steps, which are common to all problems, and equations of even complicated networks

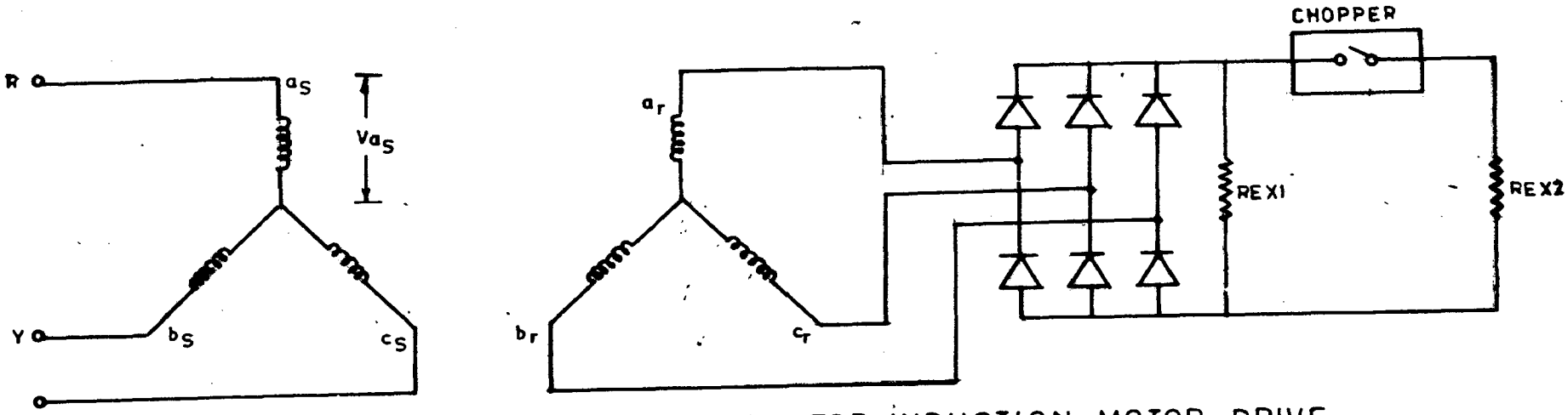

FIG. 2.1 _ ROTOR CHOPPER CONTROL FOR INDUCTION MOTOR DRIVE

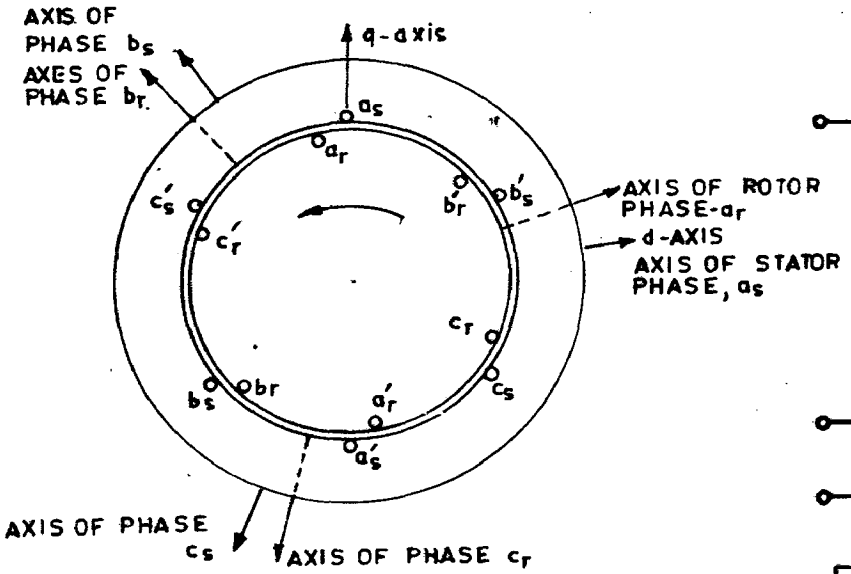

FIG. 2.2 (a) _ IDEAL 3-Ø INDUCTION MOTOR

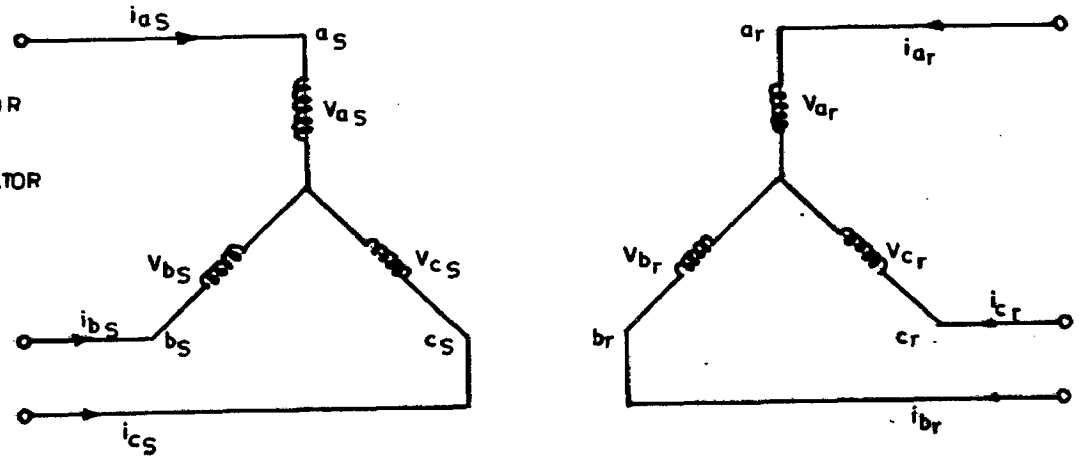

FIG. 2.2 (b) _ CONNECTIONS AND CURRENT CONVENTIONS FOR 3-Ø I MOTOR

can be easily established. For the analysis of electro-mechanical devices, it is necessary to establish equations of two parts of the system, namely the electrical systems and the mechanical systems. Thus a mathematical formulation will have -

i) a set of voltage current equations, relating the applied voltages to winding currents, using various circuit parameters.

ii) an equation of motion.

The above two sets of equations are related by a third expression which gives electromagnetic torque developed in terms of winding currents and circuit parameters.

The induction motor equations expressed in a synchronously rotating reference frame are well known to be -

Stator

$$V_{ds} = (R_1 + L_{11}p)\, i_{ds} - (wL_{11})i_{qs} + (L_{12}p)i_{dr} - (wL_{12})i_{qr} \qquad (2.1)$$

$$V_{qs} = (wL_{11})i_{ds} + (R_1 + L_{11}p)i_{qs} + (wL_{12})i_{dr} + (L_{12}p)i_{qr} \qquad (2.2)$$

Rotor

$$V_{dr} = (L_{12}p)i_{ds} - (SwL_{12})i_{qs} + (R_2 + L_{22}p)i_{dr} - (SwL_{22})i_{qr} \qquad (2.3)$$

$$V_{qr} = (SwL_{12})i_{ds} + (L_{12}p)i_{qs} + (SwL_{22})i_{dr} + (R_2 + L_{22}p)i_{qr} \qquad (2.4)$$

The electromagnetic torque developed by the induction motor in Nm is

$$T_E = \frac{3}{2} \cdot \frac{P}{2} L_{12} (i_{qs} i_{dr} - i_{ds} i_{qr}) \qquad (2.5)$$

Let the applied voltages to the stator at any instant be -

$$V_{as} = \sqrt{2}\, V_1 \cos wt$$

$$V_{bs} = \sqrt{2}\, V_1 \cos (wt - 2\pi/3)$$

$$V_{cs} = \sqrt{2}\, V_1 \cos (wt + \frac{2\pi}{3})$$

And the applied voltages to the rotor be -

$$V_{ar} = \sqrt{2}\, V_2 \cos (Swt + \theta_o)$$

$$V_{br} = \sqrt{2}\, V_2 \cos (Swt + \theta_o - \frac{2\pi}{3})$$

$$V_{cr} = \sqrt{2}\, V_2 \cos (Swt + \theta_o + \frac{2\pi}{3})$$

Where, θ_o is an arbitrary phase angle between stator and rotor phase voltages. With the position of d-axis so chosen that it coincides with phase a_s axis of stator and phase a_r axis of rotor at time t = 0, the equations for stator becomes

$$V_{ds} = \frac{2}{3} \left[V_{as} \cos wt + V_{bs} \cos(wt - \frac{2\pi}{3}) + V_{cs} \cos(wt + \frac{2\pi}{3}) \right]$$

By putting the values of V_{as}, V_{bs}, V_{cs} in above equation we get

$$V_{ds} = \frac{2}{3} \left[\sqrt{2}\, V_1 \cos(wt) \cos(wt) + \sqrt{2}\, V_1 \cos(wt - \frac{2\pi}{3}) \cdot \cos(wt - \frac{2\pi}{3}) \right.$$

$$\left. + \sqrt{2}\, V_1 \cos(wt + \frac{2\pi}{3}) \cdot \cos (wt + \frac{2\pi}{3}) \right]$$

$$= \sqrt{2}\, V_1 \cdot \frac{2}{3} \left[\cos^2(wt) + \cos^2(wt - \frac{2\pi}{3}) + \cos^2(wt + \frac{2\pi}{3}) \right]$$

$$= \sqrt{2}\, V_1$$

Similarly for q-axis

$$V_{qs} = -\frac{2}{3}\cdot\sqrt{2}\ V_1 \left[\cos wt \cdot \sin wt + \cos\left(wt - \frac{2\pi}{3}\right)\cdot \sin\left(wt - \frac{2\pi}{3}\right) + \cos\left(wt + \frac{2\pi}{3}\right)\cdot \sin\left(wt + \frac{2\pi}{3}\right)\right]$$

which after simplification gives

$$V_{qs} = 0$$

and since in plain induction motor rotor windings are short circuited

$$V_{dr} = 0$$
$$V_{qr} = 0$$

Now substituting the value of $V_{ds}, V_{qs}, V_{dr}, V_{qr}$ in equations (2.1)- (2.4)

$$\sqrt{2}\ V_1 = (R_1 + L_{11}p)\ i_{ds} - (wL_{11})i_{qs} + (L_{12}p)i_{dr} - (wL_{12})i_{qr} \quad (2.6)$$

$$0 = (wL_{11})i_{ds} + (R_1 + L_{11}p)i_{qs} + (wL_{12})\ i_{dr} + (L_{12}p)i_{qr} \quad (2.7)$$

$$0 = (L_{12}p)i_{ds} - (SwL_{12})i_{qs} + (R_2 + L_{22}p)\ i_{dr} - (SwL_{22})i_{qr} \quad (2.8)$$

$$0 = (SwL_{12})i_{ds} + (L_{12}p)i_{qs} + (SwL_{22})i_{qr} + (R_2 + L_{22}p)i_{qr} \quad (2.9)$$

$$T_E = \frac{3}{2}\cdot\frac{p}{2}\cdot L_{12}\,(i_{qs}\, i_{dr} - i_{ds}\, i_{qr}) \quad (2.10)$$

These equations can be written in matrix form

$$\begin{bmatrix} \sqrt{2}\ V_1 \\ 0 \\ 0 \\ 0 \end{bmatrix} = \begin{bmatrix} (R_1+L_{11}p) & -wL_{11} & L_{12}p & -wL_{12} \\ wL_{11} & (R_1+L_{11}p) & wL_{12} & L_{12}p \\ L_{12}p & -SwL_{12} & (R_2+L_{22}p) & -SwL_{22} \\ SwL_{12} & L_{12}p & SwL_{22} & (R_2+L_{22}p) \end{bmatrix} \begin{bmatrix} i_{ds} \\ i_{qs} \\ i_{dr} \\ i_{qr} \end{bmatrix} \qquad (2.11)$$

2.2.2 Equations for Uncontrolled Bridge Rectifier

Assuming chopper frequency high and negligible ripple in the d.c. current, the rotor current is approximately composed of alternating square pulse of $\frac{2\pi}{3}$ duration, the average rectified current I_{dc} is related to rotor rms current I_2 by -

$$I_2^2 = 2\ \frac{I_{dc}^2}{3} \qquad (2.12)$$

The rotor rms current I_2 is related to fundamental of rotor current by

$$I_{21} = \frac{3}{\pi} I_2$$

Where, I_{21} is the rms value of fundamental compoment of rotor current. The proofs of above two equations are included in Appendix-5.

The power loss in the dc side of the rectifier bridge, under per phase consideration, becomes $I_{DC}^2 \cdot R_{eq}/3a^2$. From equation (2.12), this is equivalent to the power dissipation caused by the flow of I_2 in a resistance $0.5\ R_{eq}$ in each rotor phase. The balance of power in each rotor phase gives -

$$E_2 I_{21} \cos \theta_1 = R_2 I_2^2 + 0.5 \frac{R_{eq}}{a^2} I_2^2 + P_{mech}$$

Where I_{21} is the fundamental of the rotor current in rms, θ_1 is the angle between E_2 and I_{21}, and P_{mech} is the mechanical power. If the mechanical torque is caused by the rotor fundamental current then P_{mech} is given by -

$$P_{mech} = \left[R_2 + 0.5 \frac{R_{eq}}{a^2} \right] I_{21}^2 \ (1-s)/s$$

Hence

$$E_2 I_{21} \cos \theta_1 = R_2 I_2^2 + 0.5 \frac{R_{eq}}{a^2} \cdot I_2^2 + \left[R_2 + 0.5 \frac{R_{eq}}{a^2} \right] I_{21}^2 (1-s)/s$$

or

$$= R_2 \cdot (\pi/3)^2 I_{21}^2 + 0.5 \frac{R_{eq}}{a^2} (\pi/3)^2 I_{21}^2 + \left[R_2 + 0.5 \frac{R_{eq}}{a^2} \right] I_{21}^2 \frac{(1-s)}{s}$$

$$= \left(\frac{\pi^2}{9} - 1 \right) \left(R_2 + 0.5 \frac{R_{eq}}{a^2} \right) I_{21}^2 + \left(R_2 + 0.5 \frac{R_{eq}}{a^2} \right) \frac{I_{21}^2}{s}$$

or

$$E'_2 I'_{21} \cos \theta_1 = \left(\frac{\pi^2}{9} - 1 \right) (R'_2 + 0.5 R_{eq}) I_{21}'^2 + (R'_2 + 0.5 R_{eq}) \frac{I_{21}'^2}{s}$$

where, $I'_{21} = I_{21}/a, \quad E'_2 = aE_2$

$$E'_2 I'_{21} \cos \theta_1 = R_H I'^2_{21} + (R'_2 + 0.5 R_{eq}) \frac{I'^2_{21}}{s}$$

The R_H factor that comes in picture because of harmonic loss due to rectification is given by

$$R_H = (\frac{\pi^2}{9} - 1)(R'_2 + 0.5 R_{eq}) \qquad (2.13)$$

$$E'_2 I'_{21} \cos \theta_1 = \frac{[\, sR_H I'^2_{21} + (R'_2 + 0.5 R_{eq}) I'^2_{21} \,]}{s}$$

$$E'_2 I'_{21} \cos \theta_1 = \frac{R_{2eq}}{s} I'^2_{21}$$

where

$$R_{2eq} = [\, R'_2 + 0.5 R_{eq} + sR_H \,] \qquad (2.14)$$

Equivalent value of resistance controlled by chopper

let

T_{ON} - Chopper's ON time

T_{OFF} - Chopper's OFF time

R_{eq} - Equivalent Resistance

T_c - Time period of chopper

Energy loss, when chopper is ON, is given by

$$I^2_{DC} \left[\frac{R_{ex1} \cdot R_{ex2}}{R_{ex1} + R_{ex2}} \right] T_{ON}$$

Energy loss, when chopper is OFF, is given by

$$I^2_{DC} R_{ex1} \cdot T_{OFF}$$

Total energy loss = $I_{DC}^2 \quad R_{eq} \cdot T_C$

or

$$I_{DC}^2 \quad R_{eq} \cdot T_C = I_{DC}^2 \left[\frac{R_{ex1} \cdot R_{ex2}}{R_{ex1} + R_{ex2}} \right] T_{ON} + I_{DC}^2 \quad R_{ex1} \cdot T_{OFF}$$

or

$$R_{eq} = \left[\frac{R_{ex1} \cdot R_{ex2}}{R_{ex1} + R_{ex2}} \right] \frac{T_{ON}}{T_C} + R_{ex1} \cdot \frac{T_{OFF}}{T_C}$$

or

$$R_{eq} = R_{ex1} \left[1 - \delta \cdot R_{ex1} / (R_{ex1} + R_{ex2}) \right] - \qquad (2.15)$$

where, $\delta = \frac{T_{ON}}{T_C}$

2.3 EQUATIONS IN PER UNIT SYSTEM

In the present development, a per-unit notation has been adopted because of its numerous advantages -

i) A simple inspection of the per unit parameters immediately reveals much more about the basic nature of the machine than may be observed from the ordinary parameters.

ii) The numerical range of per unit parameters is small which is valuable for solution by digital computer.

iii) Arbitrary numerical factors which may appear in the ordinary equations in d-q axes transformations are avoided.

The choice of the base values for various quantities is made so that the computational effort is reduced. The base values chosen (Appendix-1) are as follows.

Unit voltage = V_{base} = Peak value of rated phase voltage in volts. = 325 volts.

Unit current = I_{base} = Peak value of rated phase current in Amps. = 10.6 Amps.

Unit impedance = $Z_{base} = \frac{V_{base}}{I_{base}}$, ohms = 30.66 ohms

Unit power = P_{base} = Rated apparent power

$$= \frac{3}{2} \cdot V_{base} \cdot I_{base} \text{ Watts}$$

$$= 5.175 \text{ KW}$$

Unit frequency = f_b = Rated frequency in c/s 50 Hz

Unit electrical speed = $w_b = 2\pi f_b$ rad/sec. $= 100\pi$ rad/sec.

Unit mechanical speed = $Y_{base} = \frac{2w_b}{P}$ rad/sec. = 50 π rad/sec.

Unit torque = $T_{base} = \frac{P_{base}}{Y_{base}}$, NW-M = 33.93 NW-M

In order to convert the equations 2.10 and 2.11 in per unit system, all quantities present in this equation must be converted to per unit by dividing them with their base values.

$$\frac{\sqrt{2}\,V_1}{V_{base}} = (R_1 + \frac{w_b}{w_b} L_{11}p)\,\frac{i_{ds}}{I_{base}} \cdot \frac{I_{base}}{V_{base}} - (\frac{w_b}{w_b} wL_{11})\,\frac{i_{qs}}{I_{base}} \cdot$$

$$\frac{I_{base}}{V_{base}} + (\frac{w_b}{w_b} L_{12}p)\,\frac{a}{a} \cdot \frac{i_{dr}}{I_{base}} \cdot \frac{I_{base}}{V_{base}} - (\frac{w_b}{w_b} wL_{12})\,\frac{a}{a} \cdot$$

$$\frac{i_{qr}}{I_{base}} \cdot \frac{I_{base}}{V_{base}}$$

$$\frac{\sqrt{2}\,V_1}{V_{base}} = (R_1 + w_b \frac{L_{11}p}{w_b})\,\frac{i_{ds}}{I_{base}} \cdot \frac{I_{base}}{V_{base}} - (w_b L_{11} \cdot \frac{w}{w_b})$$

$$\frac{i_{qs}}{I_{base}} \cdot \frac{I_{base}}{V_{base}} + (aw_b L_{12} \frac{p}{w_b})\,\frac{i_{dr}}{a\,I_{base}} \cdot \frac{I_{base}}{V_{base}}$$

$$-(aw_b L_{12} \cdot \frac{w}{w_b}) \cdot \frac{i_{qr}}{aI_{base}} \cdot \frac{I_{base}}{V_{base}}$$

$$V_1(p.u.) = (R_1(p.u) + X_{11}(p.u.)\,\frac{p}{w_b})\,i_{ds}(p.u.) - (X_{11}(p.u.) \cdot F_R) \cdot$$
$$i_{qs}(p.u.) + (X_M(p.u.)\,\frac{p}{w_b})\,i'_{dr}(p.u.) - (X_M \cdot F_R)\,i'_{qr}(p.u.)$$

where i'_{dr} and i'_{qr} are the currents referred to the stator side.

$$i'_{dr} = \frac{i_{dr}}{a}, \quad i'_{qr} = \frac{i_{qr}}{a}, \quad X_M = w_b a\, L_{12}$$

$$X_{11} = w_b L_{11}, \; X_{22} = w_b L_{22}$$

and $F_R = \frac{w}{w_b} = \frac{2\pi f}{2\pi f_b}$ is called the frequency ratio

and may also be interpreted as the applied frequency expressed in per unit. The frequency ratio F_R is defined as the ratio of applied frequency to base frequency, and base frequency has been selected as 50 Hz. This will provide a simple means of predicting the behaviour of an induction motor at any operating frequency.

Similarly the other equations can be written in p.u. system as

$$0 = F_R X_{11}\, i_{ds} + \left(R_1 + X_{11}\frac{p}{w_b}\right) i_{qs} + F_R X_M\, i'_{dr} + X_M \frac{p}{w_b}\, i'_{qr}$$

$$0 = X_M \frac{p}{w_b}\, i_{ds} - SF_R X_M\, i_{qs} + \left(R'_2 + X'_{22}\frac{p}{w_b}\right) i'_{dr} - SF_R X'_{22}\, i'_{qr}$$

$$0 = SF_R X_M\, i_{ds} + X_M \frac{p}{w_b}\, i_{qs} + SF_R\, X'_{22}\, i'_{dr} + \left(R'_2 + X'_{22}\frac{p}{w_b}\right) i'_{qr}$$

Final equations of induction motor expressed in p.u. system can be written in matrix form as

$$\begin{bmatrix} V_1 \\ 0 \\ 0 \\ 0 \end{bmatrix} = \begin{bmatrix} \left(R_1 + X_{11}\frac{p}{w_b}\right) & -F_R X_{11} & X_M \frac{p}{w_b} & -F_R X_M \\ F_R X_{11} & \left(R_1 + X_{11}\frac{p}{w_b}\right) & F_R X_M & X_M \frac{p}{w_b} \\ X_M \frac{p}{w_b} & -SF_R X_M & \left(R'_2 + X'_{22}\frac{p}{w_b}\right) & -SF_R X'_{22} \\ SF_R X_M & X_M \frac{p}{w_b} & SF_R X'_{22} & \left(R'_2 + X'_{22}\frac{p}{w_b}\right) \end{bmatrix} \begin{bmatrix} i_{ds} \\ i_{qs} \\ i'_{dr} \\ i'_{qr} \end{bmatrix} \qquad (2.16)$$

Similarly the electromagnetic torque equation (2.10) is converted in to p.u. system by dividing all quantities in this equation with their base values.

$$\frac{T_E}{T_{base}} = \frac{1}{T_{base}} \cdot \frac{3}{2} \cdot \frac{p}{2} \cdot L_{12} (i_{qs} i_{dr} - i_{ds} i_{qr})$$

$$= \left(\frac{Y_{base}}{P_{base}}\right) \cdot \frac{3}{2} \cdot \frac{p}{2} \cdot L_{12} (i_{qs} i_{dr} - i_{ds} i_{qr})$$

$$= \left(\frac{2w_b}{p} \cdot \frac{2}{3} \cdot \frac{1}{V_{base} \cdot I_{base}}\right) \cdot \frac{3}{2} \cdot \frac{p}{2} L_{12} (i_{qs} i_{dr} - i_{ds} i_{qr})$$

$$= \frac{w_b}{V_{base} \cdot I_{base}} \cdot \frac{a}{a} \cdot \frac{I_{base}}{I_{base}} L_{12} (i_{qs} i_{dr} - i_{ds} i_{qr})$$

$$= \frac{a w_b L_{12}}{V_{base}/I_{base}} \cdot \frac{1}{a (I_{base} \cdot I_{base})} (i_{qs} i_{dr} - i_{ds} i_{qr}) .$$

$$T_E \text{ (p.u.)} = X_M \text{(p.u.)} \cdot (i_{qs} i'_{dr} - i_{ds} i'_{qr}) \qquad (2.17)$$

If rotor of induction motor is connected to 3- ϕ bridge rectifier and dc terminals are connected to the chopper with external resistance, then R'_2 can be replaced by R_{2eq}, which is defined by equation (2.14). And the matrix form will be as follows.

$$\begin{bmatrix} V_1 \\ 0 \\ 0 \\ 0 \end{bmatrix} = \begin{bmatrix} (R_1 + X_{11}\frac{p}{w_b}) & -F_R X_{11} & X_M \frac{p}{w_b} & -F_R X_M \\ F_R X_{11} & (R_1 + X_{11}\frac{p}{w_b}) & F_R X_M & X_M \frac{p}{w_b} \\ X_M \frac{p}{w_b} & -SF_R X_M & (R_{2eq} + X'_{22}\frac{p}{w_b}) & -SF_R X'_{22} \\ SF_R X_M & X_M \frac{p}{w_b} & SF_R X'_{22} & (R_{2eq} + X'_{22}\frac{p}{w_b}) \end{bmatrix} \begin{bmatrix} i_{ds} \\ i_{qs} \\ i'_{dr} \\ i'_{qr} \end{bmatrix} \qquad (2.18)$$

Hence the above four equations represented by (2.18) and the torque equation given by (2.17) completely describe the behaviour of a chopper controlled slip ring induction motor. In these equations various quantities are expressed in their per-unit values. In all further developments, only the above equations expressed in per-unit system have been used. These equations can easily be handled for studying the steady state and transient behaviour of the system.

CHAPTER-III

STEADY STATE ANALYSIS

The steady state analysis of the plain and chopper controlled induction motor has been investigated in this chapter. Expressions for torque, supply current, power factor, efficiency are derived using the mathematical model developed in Chapter II. Steady state performance of a system is computed using these expressions.

3.1 INTRODUCTION

The idealised model developed on the concept of coupled circuit approach is well suited for determining the dominant features of this system. The parameters involved in the model are such that they can be easily measured at the terminals of the machine. The plain induction motor is a particular case of chopper controlled induction motor obtained with chopper duty cycle taken as unity and external resistance reduced to zero. Performance of both the chopper controlled induction motor and plain induction motor have been computed and the results of plain induction motor have been compared with experimental results.

3.2 STEADY STATE EQUATIONS

The generalised equations describing the behaviour of the plain and chopper controlled induction motor are developed in the previous chapter. During steady state operation under

balanced conditions, the system voltages and currents referred to a synchronously rotating reference frame are constant. Thus the steady state equations of the system are obtained from the equations(2.16) by setting the time rate of change of all currents equal to zero. Hence the final steady state equations for plain induction motor are

$$\begin{bmatrix} V_1 \\ 0 \\ 0 \\ 0 \end{bmatrix} = \begin{bmatrix} R_1 & -F_R X_{11} & 0 & -F_R X_M \\ F_R X_{11} & R_1 & F_R X_M & 0 \\ 0 & -SF_R X_M & R'_2 & -SF_R X'_{22} \\ SF_R X_M & 0 & SF_R X'_{22} & R'_2 \end{bmatrix} \begin{bmatrix} i_{ds} \\ i_{qs} \\ i'_{dr} \\ i'_{qr} \end{bmatrix} \tag{3.1}$$

$$T_E = X_M(i_{qs} \cdot i'_{dr} - i_{ds} \cdot i'_{qr}) \tag{3.2}$$

Similarly equations for chopper controlled slip ring induction motor can be obtained by replacing R'_2 by R_{2eq} (eq. 2.14) in equation (3.1).

Since machine parameters are known, steady state currents for different values of slip can be calculated by using the above equations. By knowing the steady state currents, electromagnetic torque can be calculated. Flow chart for steady state analysis is given in Appendix-3 and machine parameters in Appendix-2.

Supply current is given by

$$I_1 = \sqrt{\left(\frac{i_{ds}^2 + i_{qs}^2}{2}\right)} \qquad (3.3)$$

Rotor current is given by

$$I_2 = \sqrt{\left(\frac{i'^2_{dr} + i'^2_{qr}}{2}\right)} \qquad (3.4)$$

Expression for power factor, power input, mechanical output and Efficiency are

$$P_f(\text{ power factor}) = \frac{i_{ds}}{\sqrt{2}\, I_1} \qquad (3.5)$$

$$P_1 \text{ (Power input)} = V_1 \cdot I_{ds} \qquad (3.6)$$

$$P_2(\text{Mechanical output}) = T_E(1-s) \qquad (3.7)$$

$$E_{FF}(\text{Efficiency}) = \frac{P_2}{P_1} \times 100$$

3.3 ANALYTICAL RESULTS AND DISCUSSION

The performance of the system has been computed by simulating the steady state equations on a digital computer. The computed characteristics are compared with the experimental ones for plain induction motor. Similarly computed characteristics of chopper controlled induction motor can be compared with experimental ones.

3.3.1 Torque-Slip Characteristics

The electromagnetic torque developed by the system is computed using equation (3.2). The torque versus slip characteristics for different values of chopper duty cycle are as

shown in Fig.3.2. The torque/slip characteristics of Fig.(3.2) clearly indicate the range of speed control under full load condition, with chopper duty cycle as the speed control parameter. The torque/slip characteristics for plain induction motor, for different values of supply voltages are plotted in Fig.3.1. It is observed that magnitude of torque depends upon supply voltage. If it is high, torque will be high, if it is low, torque will be low.

3.3.2 Power Output- Slip Characteristics

The power output has been calculated using equation (3.7). The power output/slip curve for both plain and chopper controlled induction motor is shown in Fig.(3.3). It is seen that the power output is low under no load condition i.e. at zero slip. And as load increases power output goes on increasing up to full load condition. But the maximum value of power output, is obtained in case of plain induction motor. The value of chopper duty cycle are taken as 0.8, 0.5, 0.3.

3.3.3 Power Factor- Slip Characteristic

The power factor has been calculated for plain induction motor as well as for chopper controlled induction motor using equation (3.5). In the later case, the duty cycle is considered as 0.3, 0.5, 0.8. The curve for power factor versus slip is plotted in Figs.(3.4), (3.5),(3.6). It is observed that the power factor is poor under no load condition, and it goes on increasing, as the load increases up to full load condition.

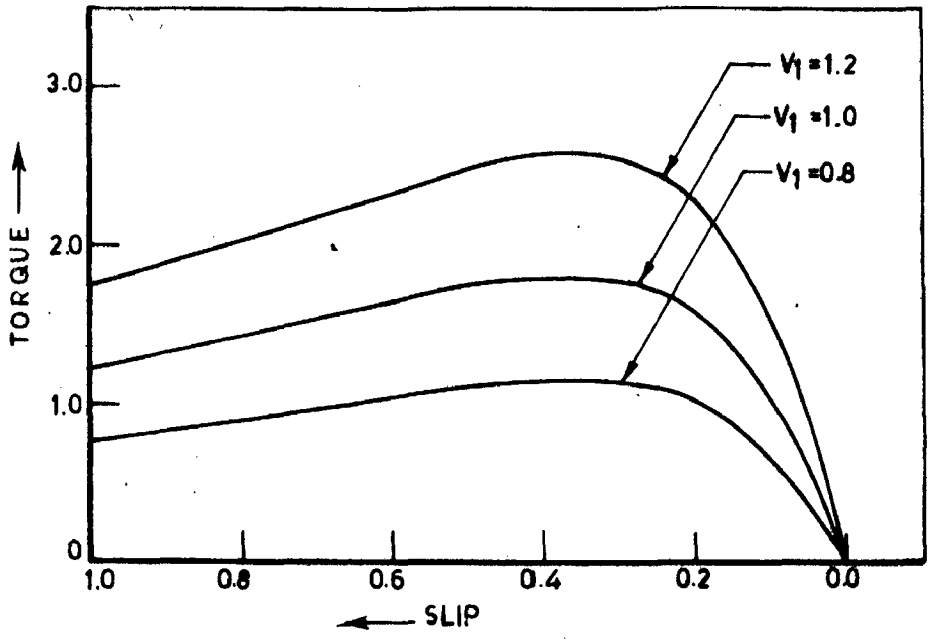

FIG. 3.1 _ TORQUE- SLIP CURVE OF PLAIN INDUCTION MOTOR

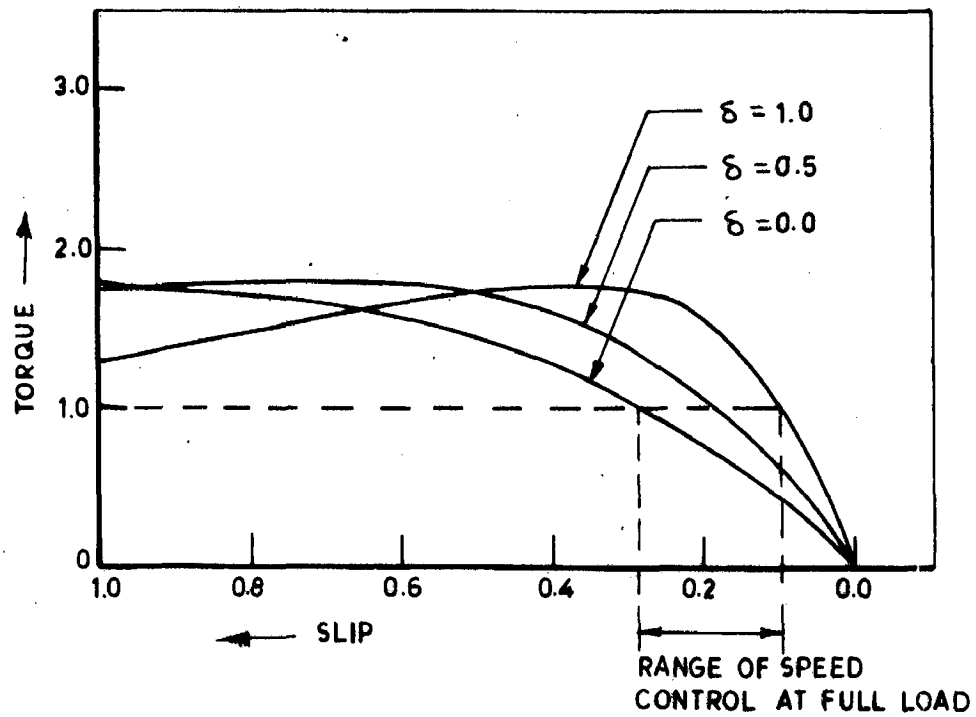

FIG. 3.2 _ TORQUE SLIP CURVE FOR CHOPPER CONTROLLED SLIP RING INDUCTION MOTOR

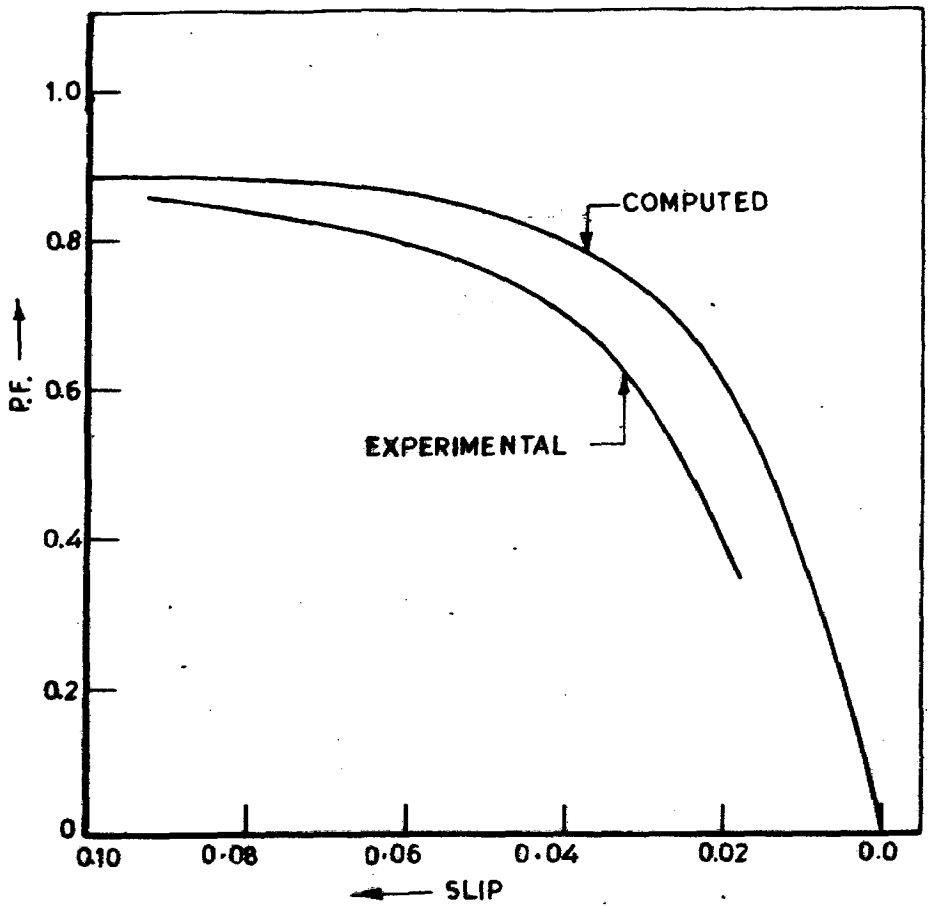

FIG. 3.4 _ POWER FACTOR-SLIP CURVES FOR PLAIN INDUCTION MOTOR [V_1=1·0]

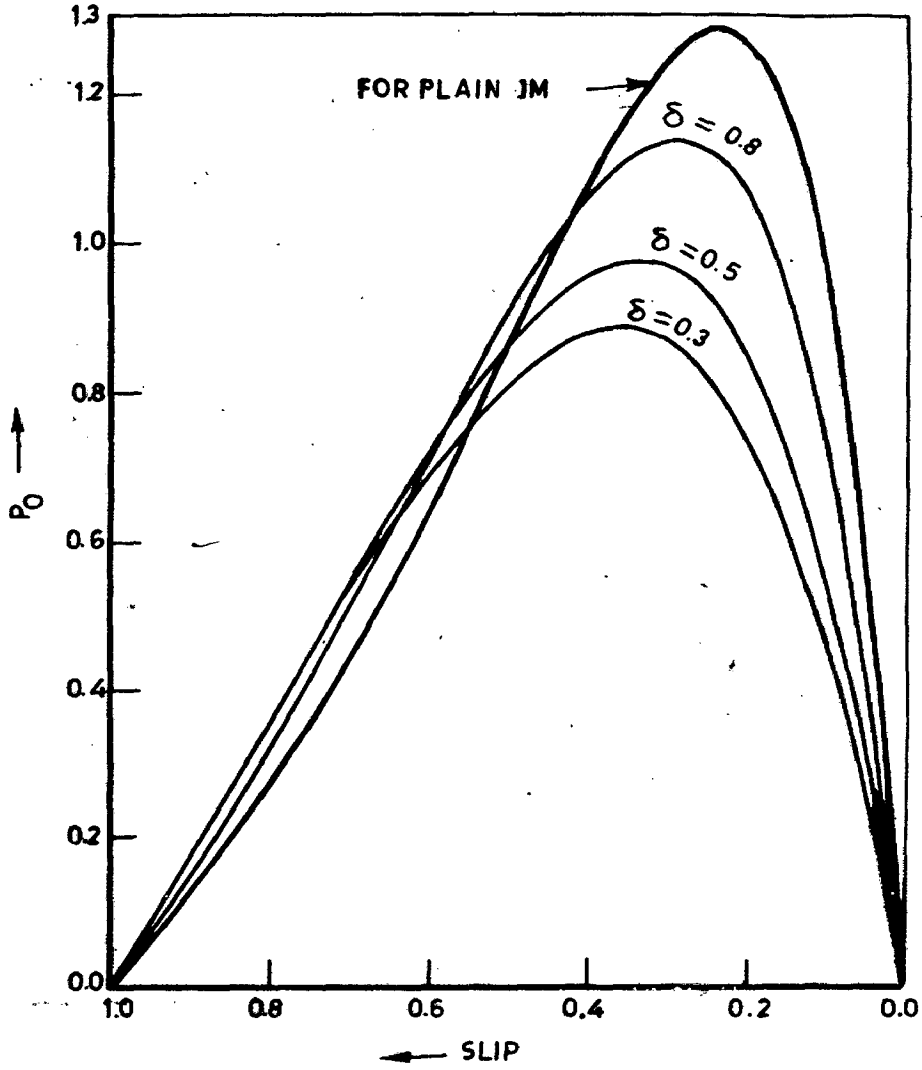

FIG. 3.3 _ POWER OUTPUT-SLIP CURVES FOR PLAIN AND CHOPPER CONTROLLED IM[V_1=1.0]

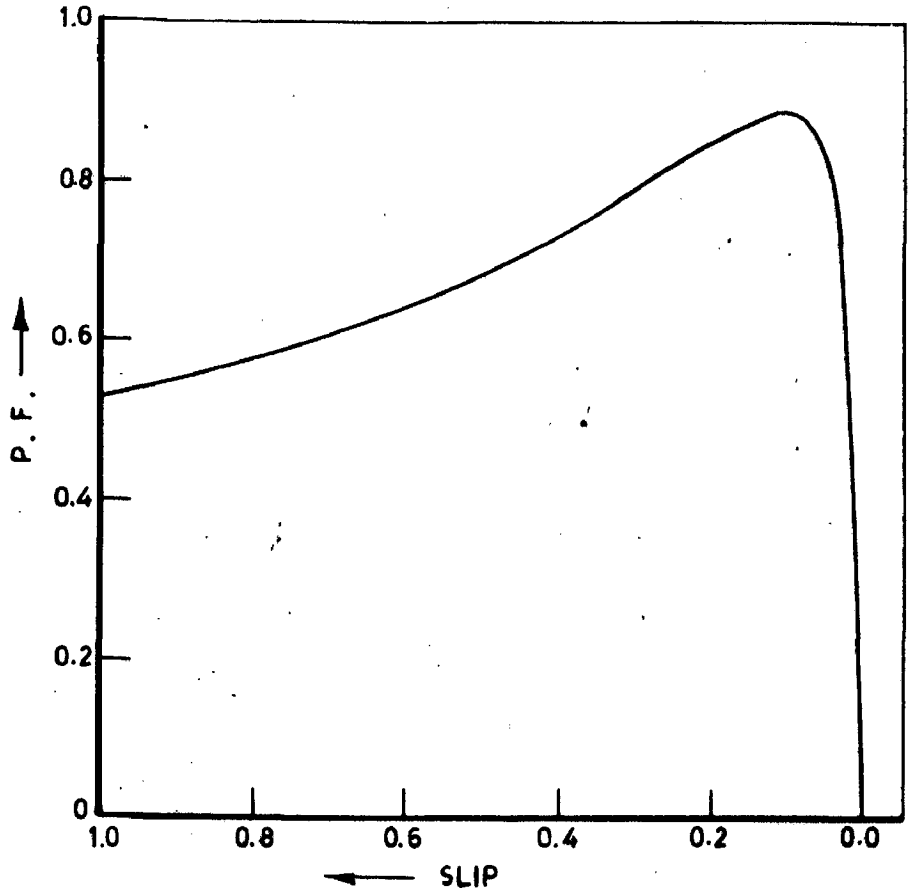

FIG. 3.5 _ POWER FACTOR - SLIP CURVE FOR PLAIN INDUCTION MOTOR [$V_1 = 1.0$]

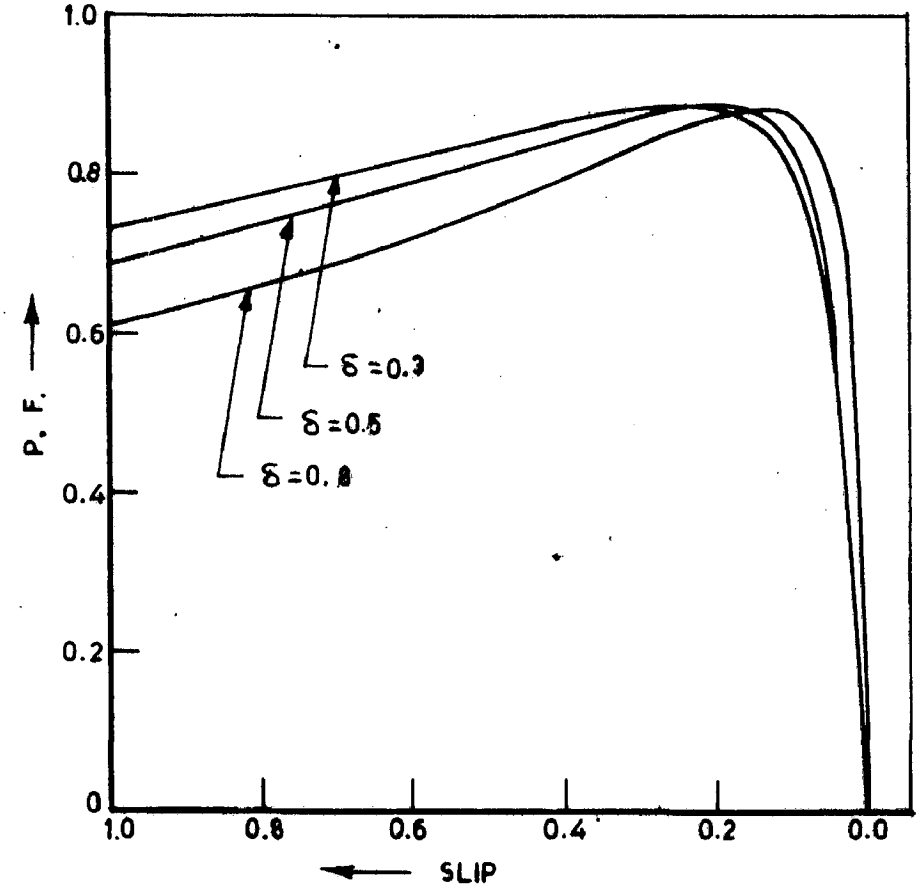

FIG. 3.6 _ POWER FACTOR-SLIP CURVE FOR CHOPPER CONTROLLED SLIP RING INDUCTION MOTOR [$V_1 = 1.0$]

3.3.4 Supply Current - Slip Curve

Figs.(3.7) and (3.8) shows the supply current versus slip characteristics for both plain and chopper controlled induction motor. In case of chopper controlled induction motor the duty cycle is taken as 0.3, 0.5, 0.8. These curves indicate that under no load condition the current is very small. And as slip increases current also increases. The starting current is greater in case of plain induction motor as compared to chopper controlled induction motor.

3.3.5 Power Input- Slip Curve

The power input has been calculated for both plain and chopper controlled induction motor using equation (3.6). In the later case, the results are obtained for the duty cycle of chopper of values 0.3, 0.5, 0.8. It is observed that under no load condition i.e. at zero slip the power input is minimum, and it goes on increasing as slip increases. The curves are shown in Figs. (3.9) and (3.10).

3.3.6. Efficiency- slip Curve

The efficiency versus slip curves are shown in Figs. (3.11) and (3.12). In case of chopper controlled induction motor the duty cycle is taken as 0.3, 0.5, 0.8. It is observed that in both cases the machine is very inefficient under no load condition. And as machine is loaded, the efficiency increases.

3.4 EXPERIMENTAL CHARACTERISTICS

In order to verify the accuracy of the computed steady state performance, test have been carried out on a plain induction motor. Experimental as well as computed results are correlated in a limited region. Power factor-slip characteristics (Fig.3.4), indicate that the measured values of power factor are less than the computed ones. In supply current slip characteristics (Fig.(3.8)), measured value of supply current is less than the computed ones. Similar is the case of power input-slip curve (Fig.(3.10)).

3.5 REASONS FOR DISCREPANCIES BETWEEN CALCULATED AND EXPERIMENTAL RESULTS

The discrepancies between the computed and experimental curves may be due to the following reasons -

i) Here, it has been assumed that all the parameters of the system remain constant. But in practice some of them will vary with the operating conditions of the system.

ii) The effect of harmonics have been neglected in the analysis of the system.

iii) The friction losses of the induction motor have been assumed constant irrespective of speed.

iv) Errors in recording and instrument errors also causes some discrepancies.

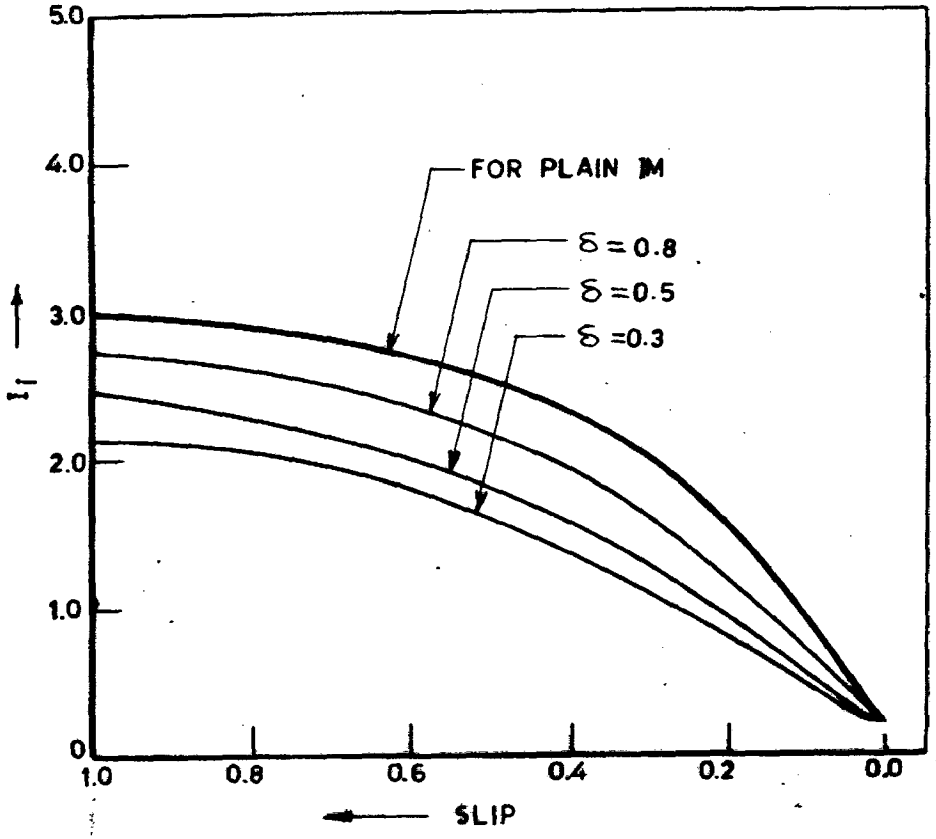

FIG. 3.7_ INPUT CURRENT- SLIP CURVE FOR PLAIN AND CHOPPER CONTROLLED IM [$V_1 = 1.0$]

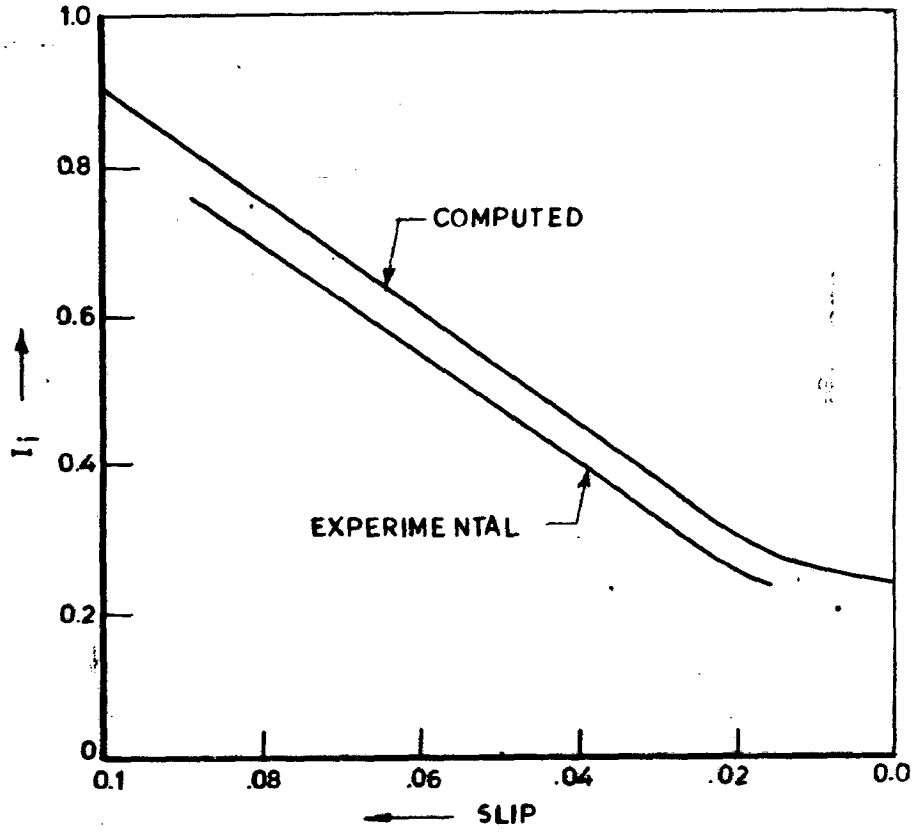

FIG. 3.8 _ INPUT CURRENT-SLIP CURVE FOR PLAIN INDUCTION MOTOR [$V_1 = 1.0$]

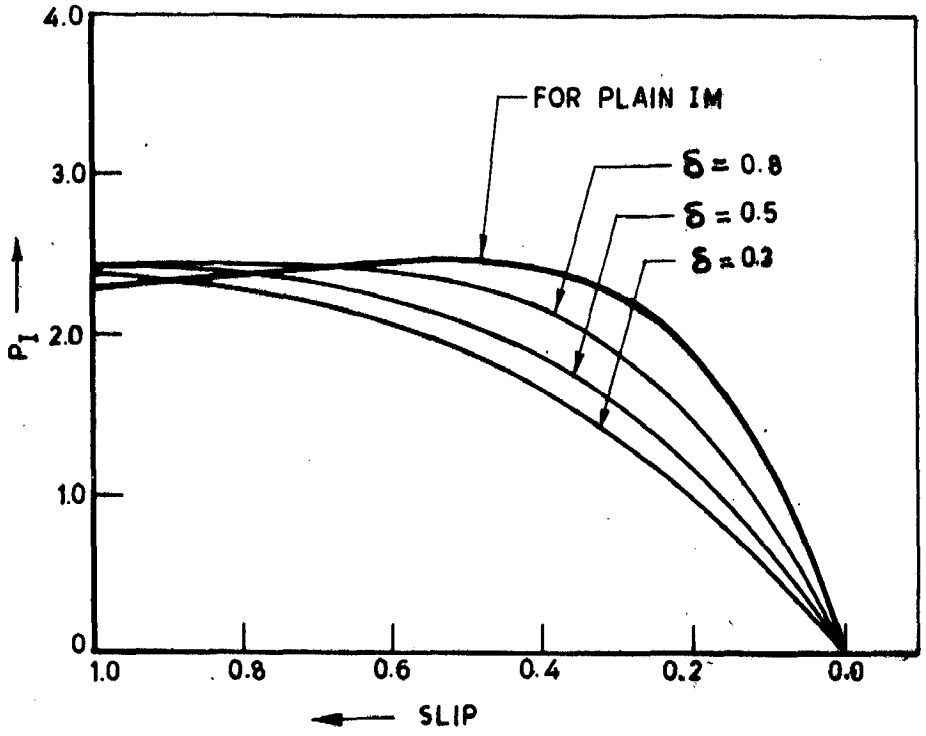

FIG. 3.9 _ POWER INPUT SLIP CURVE FOR PLAIN AND CHOPPER CONTROLLED IM [V_1 = 1.0]

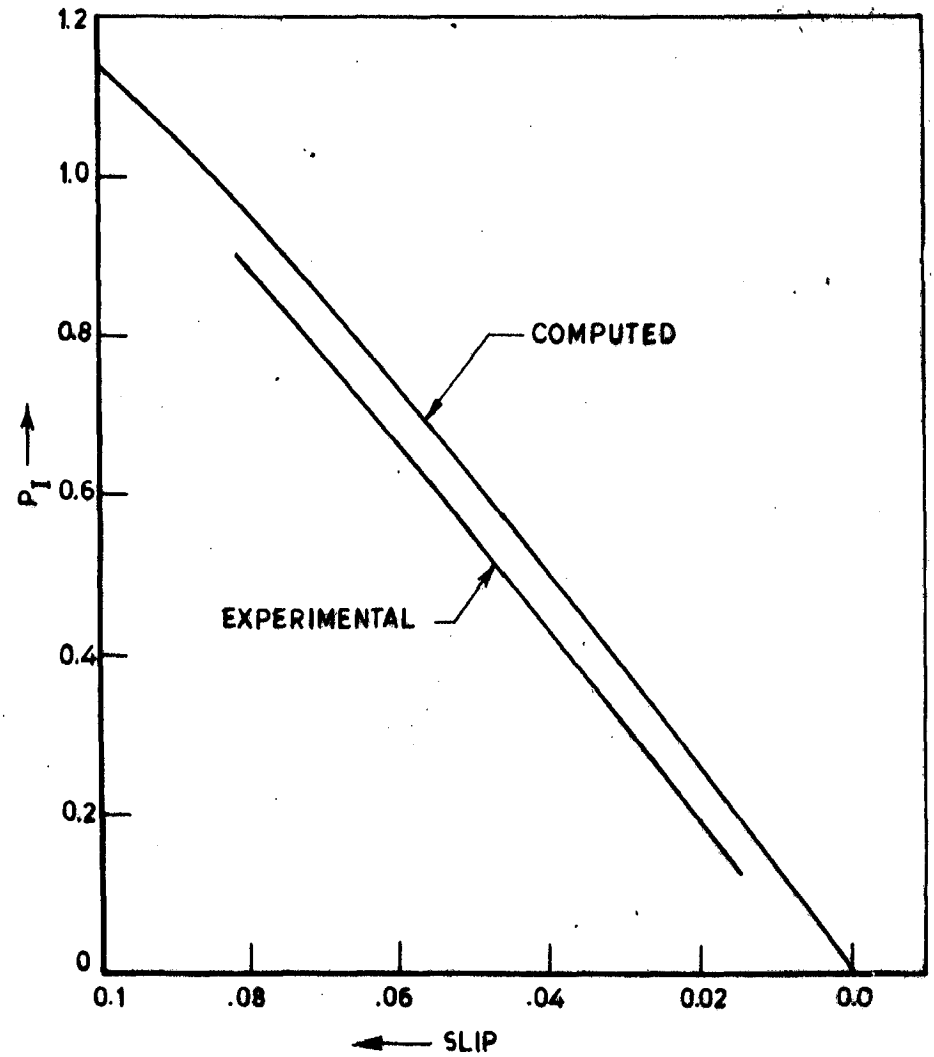

FIG. 3.10 _ POWER INPUT SLIP CURVE FOR PLAIN INDUCTION MOTOR [V_1 = 1.0]

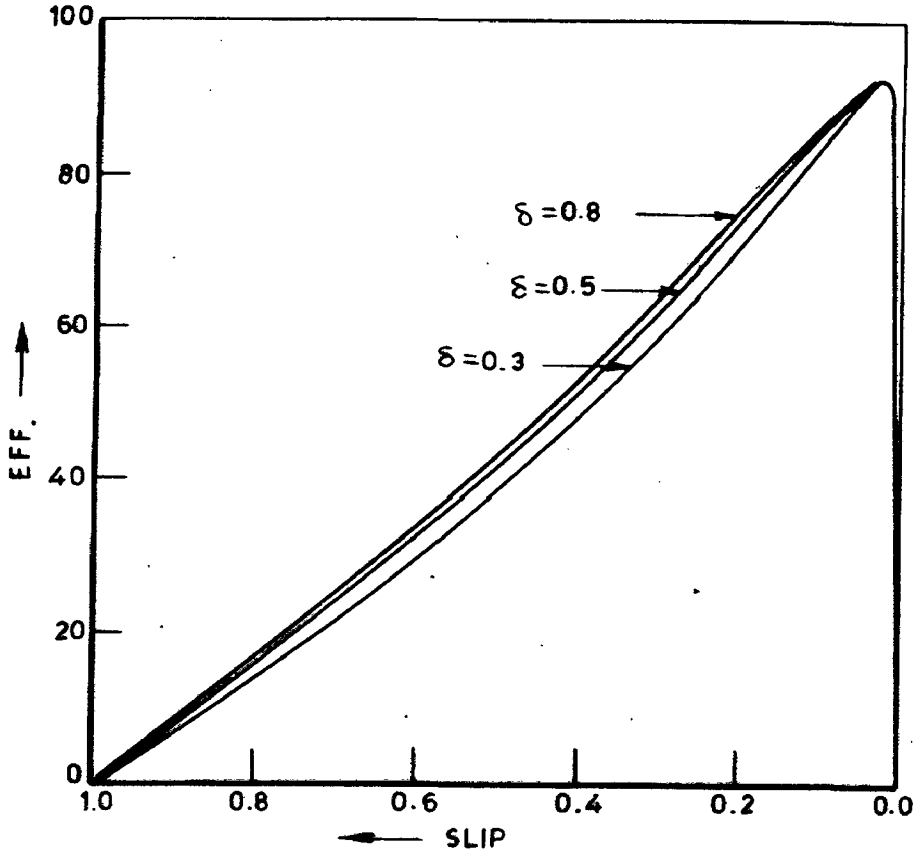

FIG. 3.11 - EFFICIENCY- SLIP CURVE FOR CHOPPER CONTROLLED INDUCTION MOTOR [$V_1 = 1.0$]

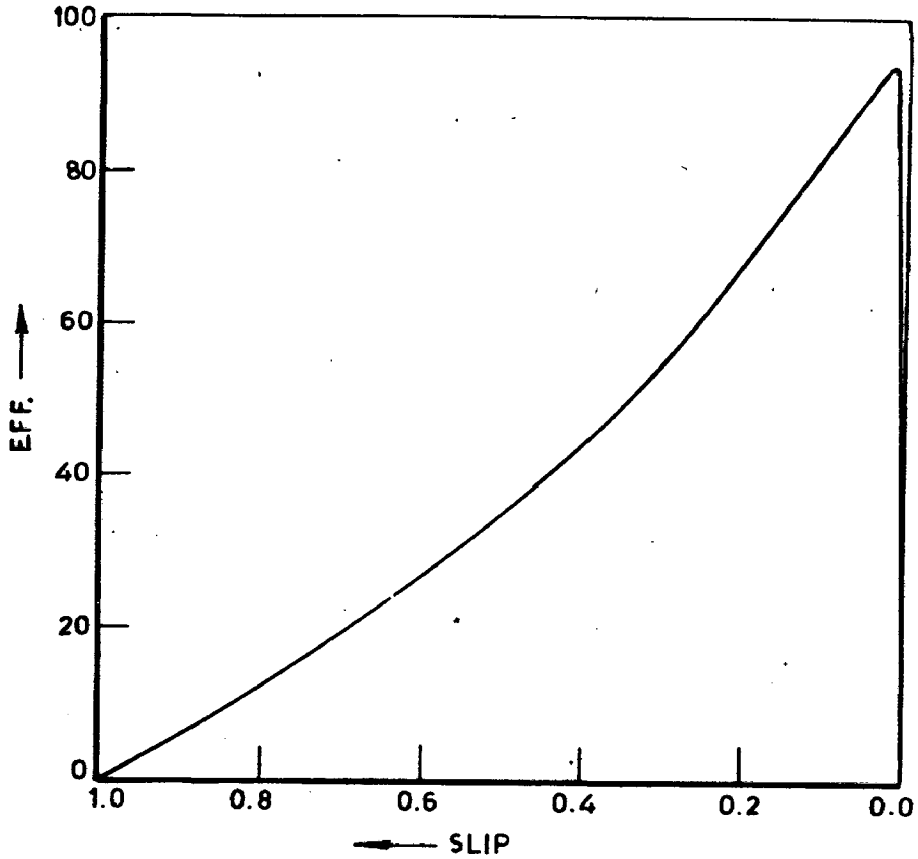

FIG. 3.12 - EFFICIENCY- SLIP CURVE FOR PLAIN INDUCTION MOTOR [$V_1 = 1.0$]

3.6 CONCLUSION

Expressions have been developed for predetermining the steady state performance of a plain and chopper controlled induction motor. The method presented is precise and quite useful for predicting accurately the operating characteristics of this system. The computed characteristics compare very closely with the experimental ones for plain induction motor. The evidence of fairly good agreement between the computed and measured results clearly justifies the expressions developed for the steady state performance.

CHAPTER-IV

SWITCHING AND RECLOSING TRANSIENTS

The satisfactory behaviour of induction motors under various electrical transient conditions is required to be guaranteed. The study enables the determination of performance variables such as torque, current, speed oscillations etc. It is increasingly becoming necessary for the manufacturers of these motors to quote figures for in-rush currents and peak torques under various transient conditions. There is also need to study the effect of variations of machine parameters on the transient performance of induction motors and modify design procedures accordingly so that optimum performance is achieved both in transient and steady state regimes. It is generally necessary to predict the phenomena by calculations based on measurable parameters of the machine, without subjecting the machine to actual transient conditions.

4.1 INTRODUCTION

The study of transient performance of static drives involving induction motors and static converters is of great practical interest, because of severe instantaneous torque generation during the transition period. Although this condition persists only for a very short time, the transient torques impose undue strain on the mechanical parts of the drive. The knowledge of transient behaviour of static drives is very

essential for the correct selection of its power capacity, the requisite power control equipment and for reducing the losses involved during transient period. The amount of energy expended during starting and reclosing is of particular importance in drives where frequent starting and reclosing is involved. Hence the investigation of the transient operating conditions and the influence upon them of various parameters is of great practical importance.

The transient behaviour of induction motors has been investigated in detail by many authors. The first papers were published in the Fourties, and a good number of papers is being published even now. For the purpose of calculating transient torque, speed has been assumed to be constant by certain investigators so that differential equations of induction machines could be solved analytically[1]. Later on analog computer was used for the study of these transients. Maginnias and Schuitz[2] have shown that the transient torque oscillations following sudden application of voltage to the machine can be much more severe than the transient torque incident to a short circuit at the motor terminals. Alger and Ku[3] also investigate the transients in induction motor when a 3-phase voltage is suddenly applied to the motor terminals. Smith, Sriharan[18], Slater, Wood[23] analysed the transient performance of induction motor by using a digital computer. They have shown that quite severe transient torques are generated following a switching operation. Lawrenson and Stephenson[19]

studied the transient performance of induction machine with a variable frequency supply. They have observed that the frequency of torque oscillations are reduced at low supply frequencies, resulting in very long settling times. The magnitude of torque peaks are reduced with a reduction in supply frequency. C.F. Landy[30] analysed the transient torque produced in an induction motor following reconnection of supply. The study of transient torques have also been carried out by many others[11,16,14,15,28,35,37]. They have simulated the dynamic equations on a digital computer and solved for the transients using Runge-Kutta method. Some of them[4,5,6,22,28,29] have also studied the reclosing transients characteristics for induction machines.

The aim of the present study is to investigate in detail the starting and reclosing transients of plain and chopper controlled induction motor under various operating conditions. A set of non-linear simultaneous differential equations describing the transient performance of the system has been developed from the generalised equations of the induction machine and from the equations of the uncontrolled rectifier bridge. These have been simulated on a digital computer and solved using Runge-Kutta method[47]. As the most important transients from the electromechanical considerations, are those of electromagnetic torques and speeds, these have been investigated under various conditions of operation.

4.2 DIGITAL SIMULATION OF SYSTEM EQUATIONS

A study of transient phenomena mostly involves determination of currents, torque, speed etc. immediately after an operational change is made. Such operations include switching-in, reclosing (or bus-transfer) and braking. In most of these studies the equations needed are four circuit equations, torque equation and equation of motion. In the analysis of these equations the impressed conditions (or forcing functions) are the four voltages V_{ds}, V_{dr}, V_{qr}, V_{qs} and the load torque T_L. The unknown variables are the four axis- currents, and the speed.

When a study of the acceleration process is required, speed has to be treated as variable. The system equations then consist of five simultaneous differential equations with variable coefficients. Such equations can be best solved by numerical methods and using digital computer. This enables direct determination of the unknown quantities corresponding to given machine parameters and initial conditions.

Equations of the system as developed in Chapter II are given below-

$$\begin{bmatrix} V_1 \\ 0 \\ 0 \\ 0 \end{bmatrix} = \begin{bmatrix} (R_1 + X_{11}\frac{p}{w_b}) & -F_R X_{11} & X_M \frac{p}{w_b} & -F_R X_M \\ F_R X_{11} & (R_1 + X_{11}\frac{p}{w_b}) & F_R X_M & X_M \frac{p}{w_b} \\ X_M \frac{p}{w_b} & -SF_R X_M & (R_{2eq} + X'_{22}\frac{p}{w_b}) & -SF_R X'_{22} \\ SF_R X_M & X_M \frac{p}{w_b} & SF_R X'_{22} & (R_{2eq} + X'_{22}\frac{p}{w_b}) \end{bmatrix} \begin{bmatrix} i_{ds} \\ i_{qs} \\ i'_{dr} \\ i'_{qr} \end{bmatrix} \quad (4.1)$$

$$T_E = X_M \, (i_{qs} \cdot i'_{dr} - i_{ds} \cdot i'_{qr}) \qquad (4.2)$$

The system of equations represented by (4.1) can be rewritten as,

$$[V] = [R]\,[i] + [X]\left[\frac{p}{w_b} i\right]$$

So that,

$$\left[\frac{p}{w_b} i\right] = -[X]^{-1}\,[R]\,[i] + [X]^{-1}\,[V] \qquad (4.3)$$

where,

$[R]$ and $[X]$ are the matrices formed by terms independent of p and coefficient of p/w_b.

$$[R] = \begin{bmatrix} R_1 & -F_R X_{11} & 0 & -F_R X_M \\ F_R X_{11} & R_1 & F_R X_M & 0 \\ 0 & -SF_R X_M & R_{2eq} & -SF_R X'_{22} \\ SF_R X_M & 0 & SF_R X'_{22} & R_{2eq} \end{bmatrix} \qquad (4.4)$$

$$[X] = \begin{bmatrix} X_{11} & 0 & X_M & 0 \\ 0 & X_{11} & 0 & X_M \\ X_M & 0 & X'_{22} & 0 \\ 0 & X_M & 0 & X'_{22} \end{bmatrix} \qquad (4.5)$$

$$[X]^{-1} = \frac{1}{A}\begin{bmatrix} X'_{22} & 0 & -X_M & 0 \\ 0 & X'_{22} & 0 & -X_M \\ -X_M & 0 & X_{11} & 0 \\ 0 & -X_M & 0 & X_{11} \end{bmatrix} \qquad (4.6)$$

Where,

$$A = [X_{11} \cdot X_{22} - X_M \cdot X_M]$$

$$[X]^{-1}[V] = \frac{1}{A}\begin{bmatrix} X'_{22} \cdot V_1 \\ 0 \\ -X_M \cdot V_1 \\ 0 \end{bmatrix}$$

$$[X]^{-1}[R] = \frac{1}{A}\begin{bmatrix} X'_{22}R_1 & (-F_R X_{11} X'_{22} + SF_R X_M^2) & -X_M R_{2eq} & (-F_R X'_{22} X_M + SF_R X'_{22} X_M) \\ (F_R X_{11} X'_{22} - SF_R X_M^2) & R_1 X'_{22} & (F_R X'_{22} X_M - SF_R X'_{22} X_M) & -R_{2eq} X_M \\ -X_M R_1 & (F_R X_{11} X_M - SF_R X_{11} X_M) & R_{2eq} X_{11} & (F_R X_M^2 - SF_R X_{11} X'_{22}) \\ (-F_R X_{11} X_M + SF_R X_{11} X_M) & -R_1 X_M & (-F_R X_M^2 + SF_R X_{11} X'_{22}) & R_{2eq} X_{11} \end{bmatrix}$$

Equation 4.3 thus implies

$$\frac{1}{w_b}\begin{bmatrix} pi_{ds} \\ pi_{qs} \\ pi'_{dr} \\ pi'_{qr} \end{bmatrix} = -\begin{bmatrix} [X]^{-1} & [R] \end{bmatrix} \begin{bmatrix} i_{ds} \\ i_{qs} \\ i'_{dr} \\ i'_{qr} \end{bmatrix} + \frac{1}{A}\begin{bmatrix} X'_{22} V_1 \\ 0 \\ -X_M V_1 \\ 0 \end{bmatrix} \qquad (4.7)$$

An additional equation of motion is obtained by considering the dynamics of the mechanical systems. During steady state condition the electromagnetic torque is equal to the load torque. However when the speed changes, the instantaneous values of electromagnetic torque T_E and load torque T_L are related by the following per unit expression

$$2H \frac{d\omega_r}{dt} = T_E - T_L$$

where $2H\, d\omega_r/dt$ is acceleration torque, H is inertia const. in sec. w_r is mechanical angular speed in pu.

or $$p\omega_r = \frac{1}{2H}\left[X_M (i_{qs} i'_{dr} - i_{ds} i'_{qr}) - T_L\right] \qquad (4.8)$$

The equations (4.7) and (4.8) are suitable for simulation and numerical integration on a digital computer. The numerical integration must enable the increments in a set of dependent variables (currents) corresponding to a small increment in the independent variable (time) to be determined, provided the

differential coefficients of the dependent variables are known with respect to the independent variable. It is therefore necessary to express the rates of change of the currents with respect to time in terms of the currents and applied voltages. Therefore the equations (4.7) and (4.8) are rewritten as a set of five non-linear simultaneous differential equations as follows -

$$p\, i_{ds} = \frac{w_b}{A}\left[-X'_{22}R_1\, i_{ds} + (F_R X_{11} X'_{22} - SF_R X_M^2)\, i_{qs} + X_M R_{2eq}\, i'_{dr} + (F_R X'_{22} X_M - SF_R X'_{22} X_M)\, i'_{qr} + X'_{22}\, V_1\right] \quad (4.9)$$

$$p\, i_{qs} = \frac{w_b}{A}\left[-(-SF_R X_M^2 + F_R\, X_{11} X'_{22})\, i_{ds} - R_1 X'_{22}\, i_{qs} - (-SF_R X'_{22} X_M + F_R X'_{22}\, X_M)\, i'_{dr} + R_{2eq}\, X_M\, i'_{qr}\right] \quad (4.10)$$

$$p\, i'_{dr} = \frac{w_b}{A}\left[X_M R_1\, i_{ds} - (-SF_R X_{11} X_M + F_R X_{11} X_M) i_{qs} - R_{2eq} X_{11} i'_{dr} - (F_R X_M^2 - SF_R X_{11}\, X'_{22})\, i'_{qr} - X_M V_1\right] \quad (4.11)$$

$$p\, i'_{qr} = \frac{w_b}{A}\left[(F_R X_{11} X_M - SF_R X_{11} X_M)\, i_{ds} + R_1 X_M i_{qs} + (F_R X_M^2 - SF_R X_{11} X'_{22})\, i'_{dr} - R_{2eq} X_{11}\, i'_{qr}\right] \quad (4.12)$$

$$pw_r = \frac{1}{2H}\left[X_M\,(i_{qs}\, i'_{dr} - i_{ds}\cdot\, i'_{qr}) - T_L\right] \quad (4.13)$$

To solve above equations efficiently, it is highly desirable to use a numerical- integration routine in which the step length can be varied to achieve reasonable accuracy. By chosing an optimum step length in the process of numerical solution, a compromise between the accuracy of the results and

the Computer time can be achieved. Runge-Kutta fourth-order method has been used to obtain starting and reclosing transients of this system. The[30] accuracy of the numerical integration depends on the integration interval, the smaller the interval the greater the accuracy. To determine the accuracy of computation, the increments in the dependent variables corresponding to a given increment in time are computed, the integration interval is then halved and the increments recalculated. This process is repeated until the last two sets of calculated increments in the dependent variables agree to within 0.1 percent. This simulation and numerical integration technique is available in the form of a ' Special Application Program' called ' Continuous System Modeling Program' (CSMP) produced by a Computer Company for use on one of their digital computers. Thus, a time increment of 0.0005 sec. is chosen for a convergent solution of adequate accuracy.

The transient currents and speed have been computed using above five non-linear simultaneous differential equations and transient torque is calculated from torque equation.

4.3 OPEN CIRCUIT CONDITIONS IN THE MOTOR

When[30] an induction motor is disconnected from the supply the air gap flux decays at a rate associated with the electrical time constant of the rotor circuit. For a short period of time following disconnection this decaying air-gap flux will cause emf's to be induced in the stator windings, having a frequency dependent on the rotor speed and, therefore,

short time depending on the characteristics of the switch, and this will be assumed here to be zero. Since the flux can not change instantaneously, a balance of mmf must be maintained over the boundary of switching. Thus the change in the stator currents must be accompanied by a corresponding change in the rotor currents thereby maintaining constant flux linkages immediately before and after switching.

The d,q currents are proportional to the mmf's produced by them so that prior to switching

$$F_d \propto i_{ds1} + i_{dr1}$$

and

$$F_q \propto i_{qs1} + i_{qr1}$$

where suffixes 1 and 2 denote the currents before and after switching.

After switching

$$F_d \propto i_{dr2}$$

$$F_q \propto i_{qr2}$$

Hence to maintain a balance of mmf during switching

$$\begin{aligned} i_{dr2} &= i_{ds1} + i'_{dr1} \\ i_{qr2} &= i_{qs1} + i'_{qr1} \end{aligned} \tag{4.16}$$

Equations (4.16) provide the boundary conditions for i_{dr} and i_{qr} required in equations (4.14) and (4.15), since these rotor currents are referred to the stator by the property

of the transformation used. These boundary conditions are necessary to determine the decay of rotor currents and stator voltages until reswitching.

DECAY OF ROTOR CURRENTS

Equation (4.15) can be written in the following form as -

$$[V] = [R]\ [i] + [X]\left[\frac{p}{w_b} i\right]$$

so that

$$\left[\frac{p}{w_b} i\right] = [X]^{-1}\left[[V] - [R]\ [i]\right]$$

or

$$\left[\frac{p}{w_b} i\right] = -\ [X]^{-1}\ [R][i] + [X]^{-1}\ [V]$$

Where $[R]$ and $[X]$ are the matrices formed by the terms independent of p and coefficients of p/w_b.

$$[V] = \begin{bmatrix} 0 \\ 0 \end{bmatrix}, \quad [R] = \begin{bmatrix} R'_{2eq} & -SF_R X'_{22} \\ SF_R X'_{22} & R'_{2eq} \end{bmatrix}, \quad [X] = \begin{bmatrix} X'_{22} & 0 \\ 0 & X'_{22} \end{bmatrix}$$

$$[i] = \begin{bmatrix} i'_{dr} \\ i'_{qr} \end{bmatrix}, \quad [X]^{-1} = \begin{bmatrix} \frac{1}{X'_{22}} & 0 \\ 0 & \frac{1}{X'_{22}} \end{bmatrix}$$

Therefore

$$\left[\frac{p}{w_b} i\right] = -\begin{bmatrix} \frac{1}{X'_{22}} & 0 \\ 0 & \frac{1}{X'_{22}} \end{bmatrix}\begin{bmatrix} R'_{2eq} & -SF_R X'_{22} \\ SF_R X'_{22} & R'_{2eq} \end{bmatrix}\begin{bmatrix} i'_{dr} \\ i'_{qr} \end{bmatrix} + \begin{bmatrix} \frac{1}{X'_{22}} & 0 \\ 0 & \frac{1}{X'_{22}} \end{bmatrix}\begin{bmatrix} 0 \\ 0 \end{bmatrix}$$

or

$$\frac{1}{w_b}\begin{bmatrix} p\, i'_{dr} \\ p\, i'_{qr} \end{bmatrix} = -\begin{bmatrix} \frac{R'_{2eq}}{X'_{22}} & -SF_R \\ SF_R & \frac{R'_{2eq}}{X'_{22}} \end{bmatrix} \begin{bmatrix} i'_{dr} \\ i'_{qr} \end{bmatrix}$$

$$p\, i'_{dr} = -w_b \left[\frac{R'_{2eq}}{X'_{22}}\, i'_{dr} - SF_R\, i'_{qr} \right]$$

$$p\, i'_{qr} = -w_b \left[SF_R\, i'_{dr} + \frac{R'_{2eq}}{X'_{22}}\, i'_{qr} \right] \qquad (4.17)$$

where, i'_{dr} and i'_{qr} are the initial values of rotor currents after disconnection. Thus

$$i'_{dr} = i_{dsl} + i'_{drl}$$

$$i'_{qr} = i_{qsl} + i'_{qrl}$$

The rate of change of current $p\,[I]$ is calculated using equation (4.17). From these, the increments in the currents corresponding to an increment in time (the step length) are calculated. Adding these increments to the initial values gives the currents, which are then used in equations (4.17) to obtain new $p\,[I]$, and the process is repeated until the specified range of time is covered.

DECAY OF STATOR VOLTAGE

Equation (4.14) can be written in the following form as

$$[V] = [R]\,[i] + [X]\left[\frac{p}{w_b}\, i\right]$$

where,

$$[R] = \begin{bmatrix} 0 & -F_R X_M \\ F_R X_M & 0 \end{bmatrix}, \quad [X] = \begin{bmatrix} X_M & 0 \\ 0 & X_M \end{bmatrix}$$

$$[i] = \begin{bmatrix} i'_{dr} \\ i'_{qr} \end{bmatrix}, \quad [V] = \begin{bmatrix} V_{dso} \\ V_{qso} \end{bmatrix}$$

Suffix o corresponds to the open circuit condition.

Thus,

$$\begin{bmatrix} V_{dso} \\ V_{qso} \end{bmatrix} = \begin{bmatrix} X_M \frac{p}{w_b} & -F_R X_M \\ F_R X_M & X_M \frac{p}{w_b} \end{bmatrix} \begin{bmatrix} i'_{dr} \\ i'_{qr} \end{bmatrix} \quad \text{---- (A)}^*$$

and open circuit voltage is given by

$$E_A = V_{dso} \cos(w_b t) - V_{qso} \sin(w_b t) \qquad (4.18)$$

DECAY OF SPEED

The electromagnetic torque equation is

$$T_E = X_M \left(i_{qs} \cdot i'_{dr} - i'_{ds} \cdot i'_{qr} \right)$$

Equation of motion is given by

$$2H \, p w_r = T_E - T_L$$

where wr is the speed of rotor in p.u.

$$p w_r = \frac{1}{2H} \left[X_M \left(i_{qs} \cdot i'_{dr} - i_{ds} \cdot i'_{qr} \right) - T_L \right]$$

Since under open circuit conditions

$$i_{ds} = i_{qs} = 0$$

$$p w_r = - \frac{1}{2H} T_L \qquad (4.19)$$

The rate of change of speed under open circuit condition can be calculated using equation (4.19).

4.4 COMPUTER PROGRAM

The initial part of the digital computer program for the numerical solution of equation 4.1 deals with connection of the inert machine to the supply, with the numerical integration based on the Runge-Kutta method.

Equation (4.1) may be rewritten in the form

$$[v] = [R][i] + [X]\left[\frac{p}{w_b} i\right]$$

and the rate of change of current with respect to time is given by

$$p[i] = w_b \left[- [X]^{-1} [R][i] + [X]^{-1} [v] \right] \qquad (4.19)$$

where $[R]$ and $[X]$ are the matrices formed by terms independent of p and coefficient of p/w_b.

With the given applied stator voltages, the initial zero stator and rotor currents and the speed, the rates of change of the current $p[i]$ are calculated using equation (4.19). From these the increments in the currents corresponding to an increment in time (the step length) are calculated using the numerical integration on a digital computer. Adding these increments to the initial values gives the currents, which are then used in equation (4.19) to obtain new $p[i]$, and the process is repeated until the specified range of time is covered. The new speed of the motor is obtained by numerical integration from the equation (4.13).

The next part of the program deals with the open circuit conditions in the motor, following disconnection from the supply. In general, equation (4.1) may be written for partition in the form

$$\begin{bmatrix} V_1 \\ V_2 \end{bmatrix} = \begin{bmatrix} Z_{11} & Z_{12} \\ Z_{21} & Z_{22} \end{bmatrix} \cdot \begin{bmatrix} i_1 \\ i_2 \end{bmatrix}$$

Where V_1 and i_1 refer to the open circuited circuits and V_2 and i_2 to the remaining circuits. Since $i_1 = 0$ on open circuit,

$$\begin{aligned} [V_1] &= [Z_{12}] \cdot [i_2] \\ &= [R_{12}][i_2] + [X_{12}] \cdot \left[\frac{p}{w_b} i_2\right] \end{aligned} \qquad (4.20)$$

Additionally

$$\begin{aligned} [V_2] &= [Z_{22}] \cdot [i_2] \\ &= [R_{22}][i_2] + [X_{22}] \cdot \left[\frac{p}{w_b} i_2\right] \end{aligned}$$

or

$$p\,[i_2] = w_b \left[- [X_{22}]^{-1} [R_{22}] [i_2] + [X_{22}]^{-1} [V_2] \right] \qquad (4.21)$$

Equation (4.21) is the same as equation (4.19), with the original matrix $[Z]$ of equation (4.1) replaced by the impedance matrix $[Z_{22}]$. In the program $[Z_{22}]$ is found by deleting the rows and columns of $[Z]$ corresponding to the opened circuits. The initial rotor currents after disconnection are found using the principle of constant flux linkage, and the subsequent decay of rotor currents and stator voltages are found by using equations (4.21) and (4.20), respectively.

For the final part of the program dealing with reswitching the impedance matrix is changed back to [z] , and the computation is performed as for connection but with the initial values determined from the open-circuit calculation. A simplified block diagram for the program is given in Fig.4.1. And the complete flow-chart for transient study is given in Appendix-4.

4.5 ANALYTICAL RESULTS AND DISCUSSION

Reclosing transients have been computed for the following cases :

(a) A plain induction motor (slip rings short circuited)

(b) A chopper controlled induction motor drive

In both cases the procedure of obtaining the reclosing transients has been as follows. The motor/drive is started from rest by applying rated voltage. The switching transients are computed till the steady state is reached. Supply is now withdrawn for a short interval (to be defined later) and the switch is again closed. The resulting transients are computed, once again, till steady state is reached.

For the case of chopper controlled induction motor drive, the chopper duty cycle has been adjusted arbitrarily at 0.5. Other values of the chopper duty cycle have also been considered in one case.

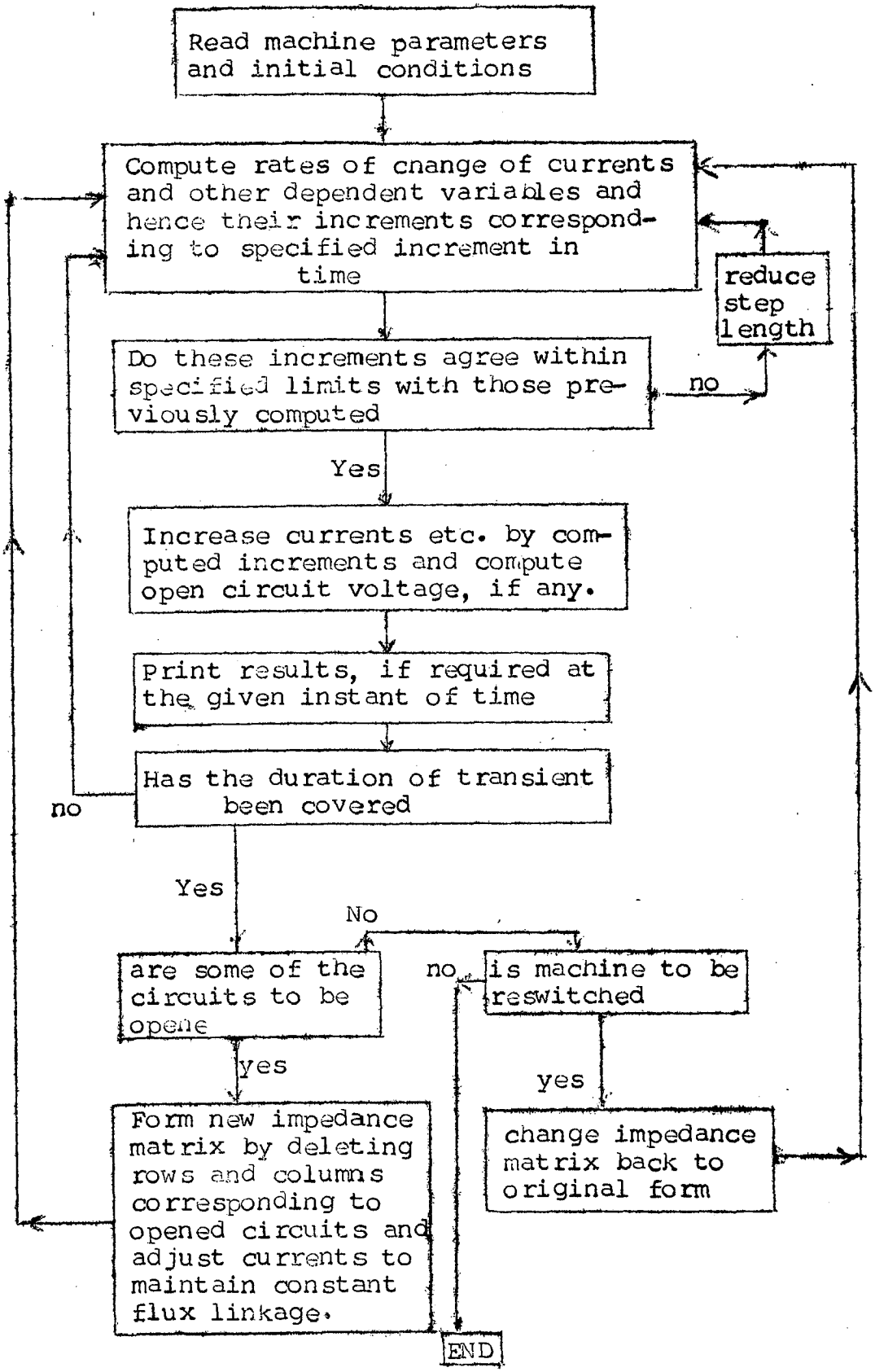

Fig.4.1 - FLOW DIAGRAM OF COMPUTER PROGRAM

4.5.1 Reclosing Transients for Plain Induction Motor

Figures 4.2(a) to 4.2 (h) present the relevant details involved in the study of reclosing transients. The induction motor is considered to have a constant load torque of 0.5 p.u., present all the time. The inertia constant is taken as 0.25 p.u. The applied voltage and frequency have normal values of 1 p.u. Normal parameters of the machine (as given in Appendix-2) are considered.

Fig. 4.2(a) shows how the open circuit voltage falls during the period of supply interruption. The supply voltage waveform is also shown alongwith to indicate the phase difference between the two voltages. It can be observed that at 0.1 sec. the values of supply voltage and open circuit voltage are 1.0 p.u. and -0.424 p.u. respectively. So that if the switch is reclosed at this instant the resultant voltage would be (1.0 - (-0.424) = 1.424 p.u.). An instant, earlier or later than this instant, the resultant voltage is found to be less than 1.424 p.u.

Fig. 4.2(b) shows the decay of speed with respect to time during the period of supply interrup-tion. It is noted that after 0.95 sec. the machine comes to rest. The open circuit voltage has also fallen to zero by this time.

Fig. 4.2(c) and (d) represent switching and reclosing transients for two different reclosing instants. Fig.4.2(c)

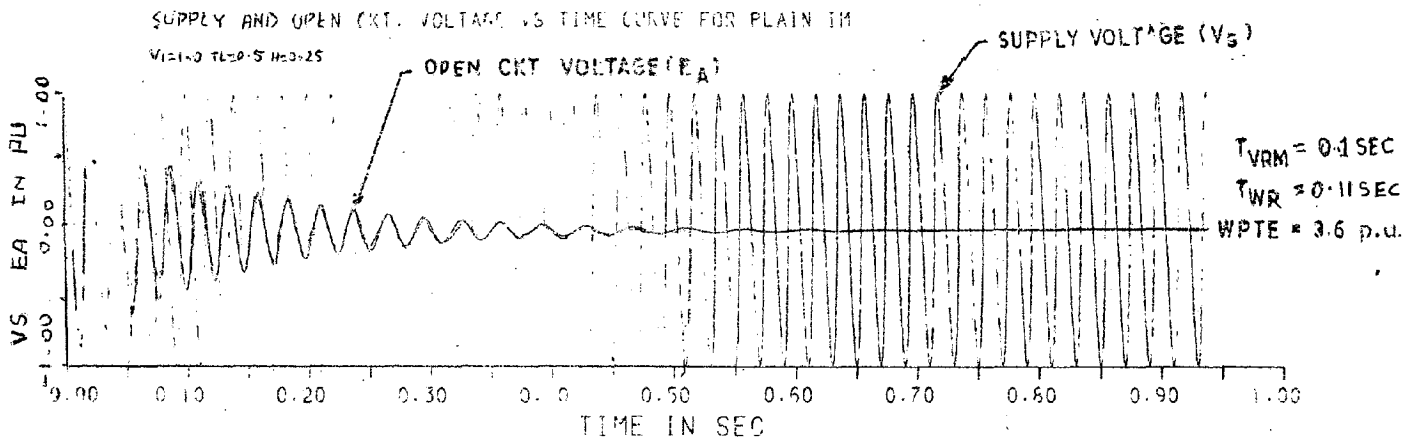

FIG. 4.2 (a)

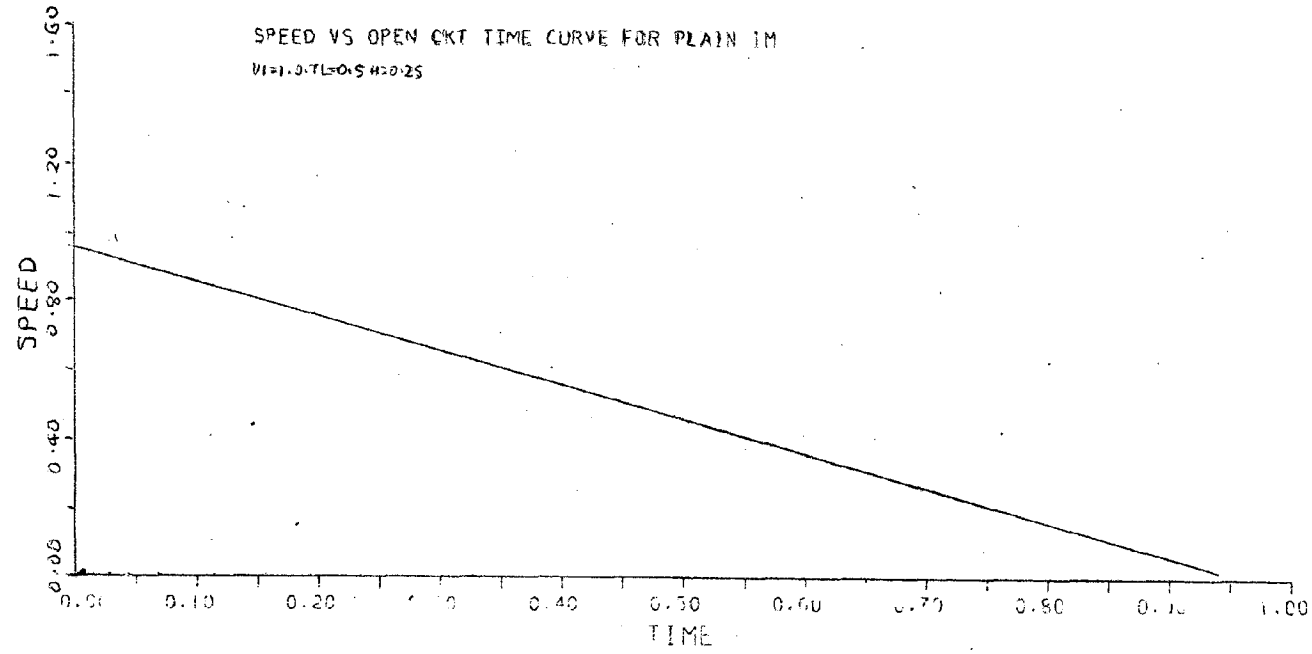

FIG. 4.2 (b)

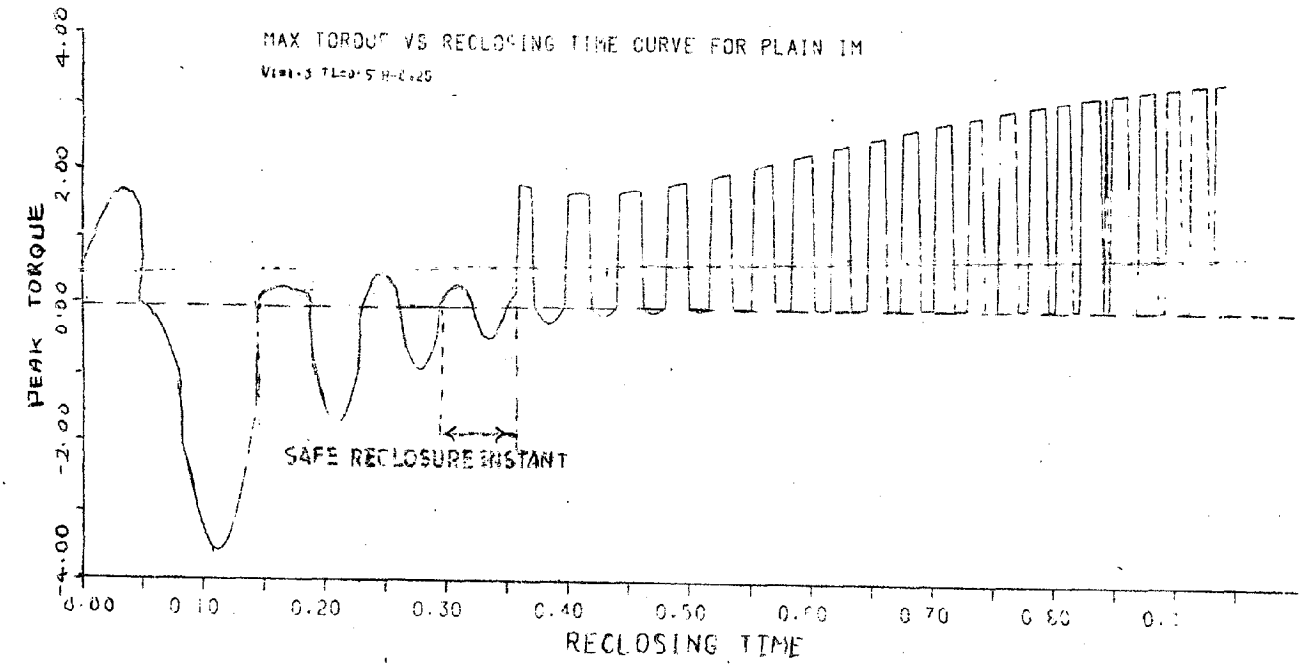

FIG. 4.2 (c)

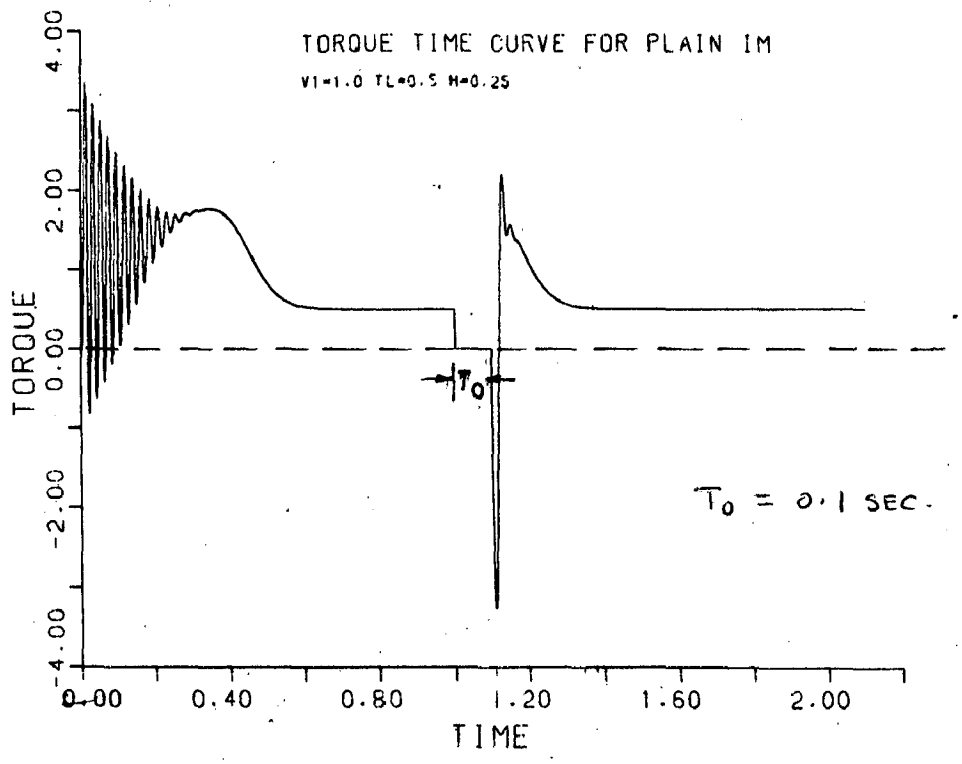

FIG. 4.2'(c)

T_0 = PERIOD OF SUPPLY INTERRUPTION

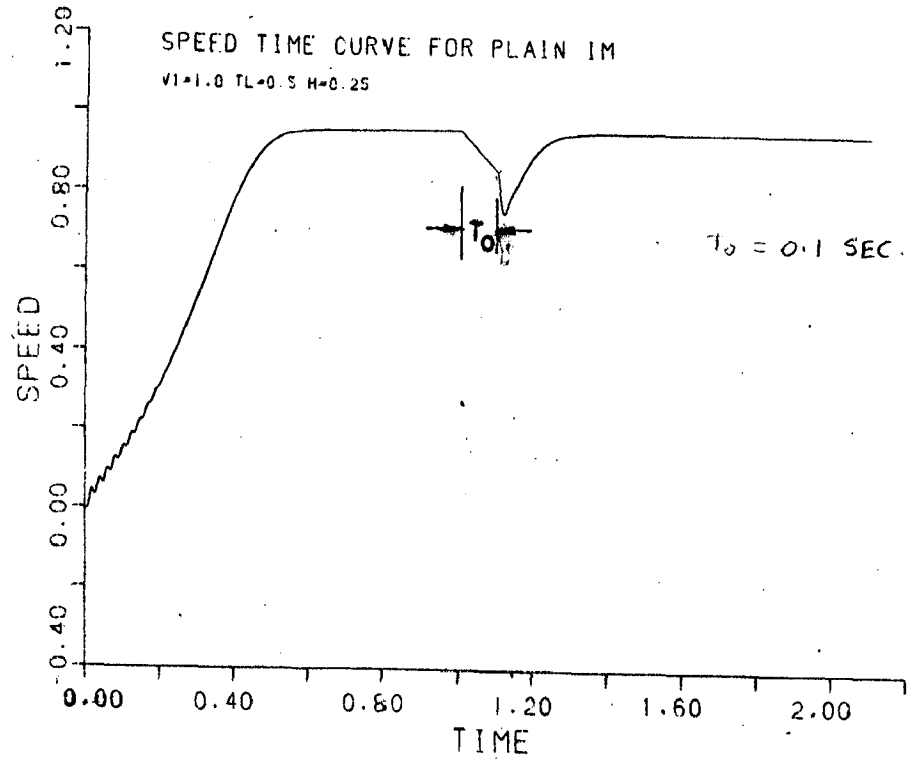

FIG. 4.2(g)

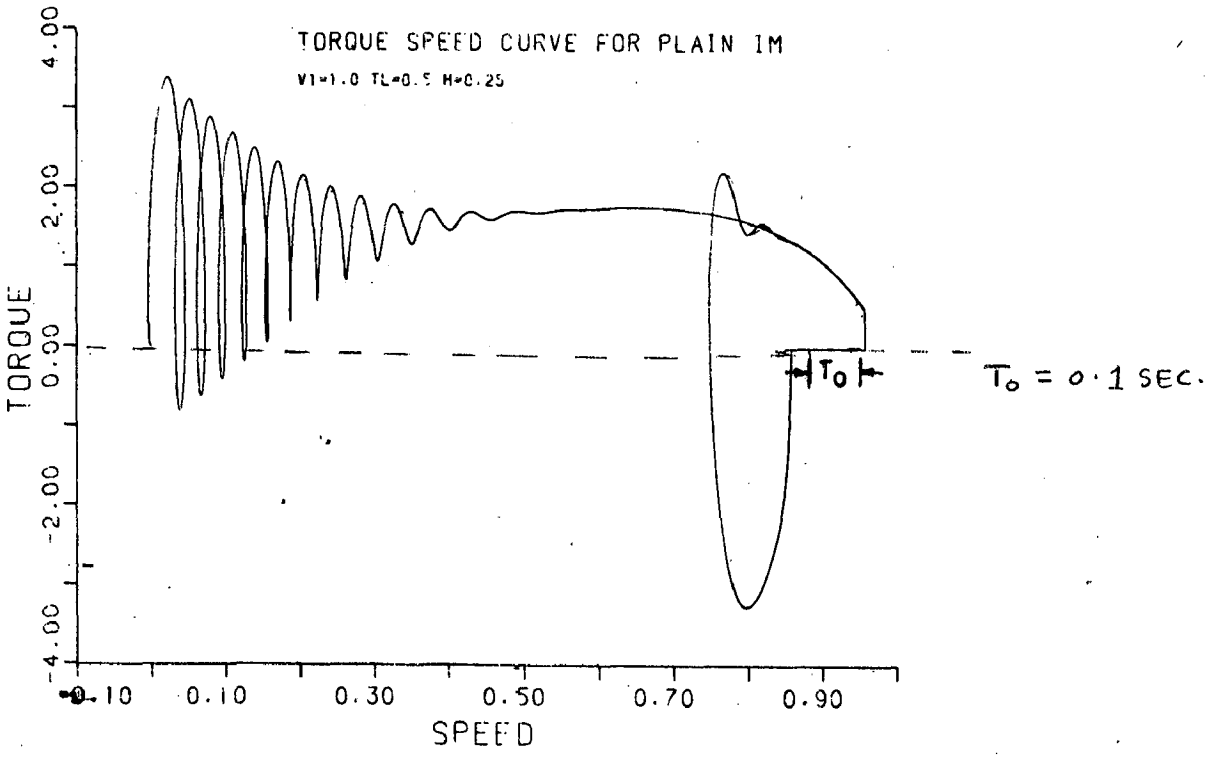
TORQUE SPEED CURVE FOR PLAIN IM
V1=1.0 TL=0.5 H=0.25
TORQUE
4.00
2.00
0.00
-2.00
-4.00
-0.10
0.10
0.30
0.50
0.70
0.90
SPEED
T_0
T_0 = 0·1 SEC.

FIG. 4.2 (h)

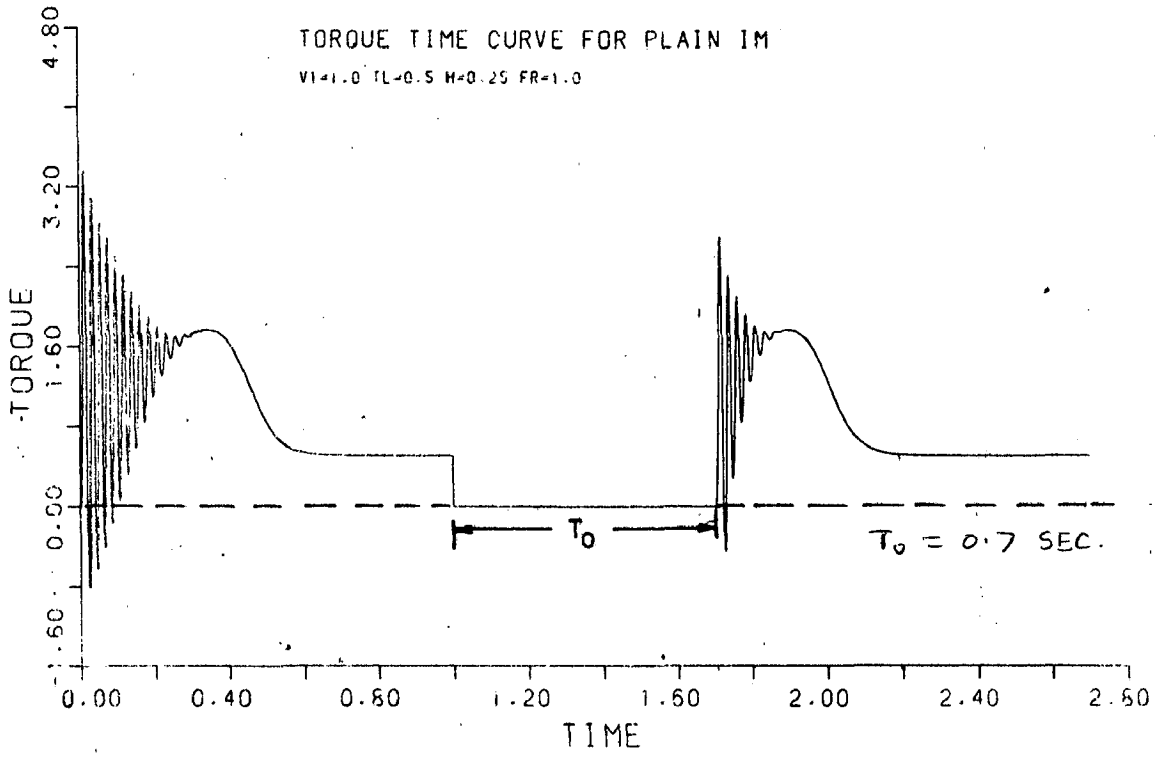
TORQUE TIME CURVE FOR PLAIN IM
VI=1.0 TL=0.5 H=0.25 FR=1.0
TORQUE
4.80
3.20
1.60
0.00
-1.60
T_0
T_0 = 0·7 SEC.
0.00
0.40
0.80
1.20
1.60
2.00
2.40
2.80
TIME

FIG. 4.2(d)

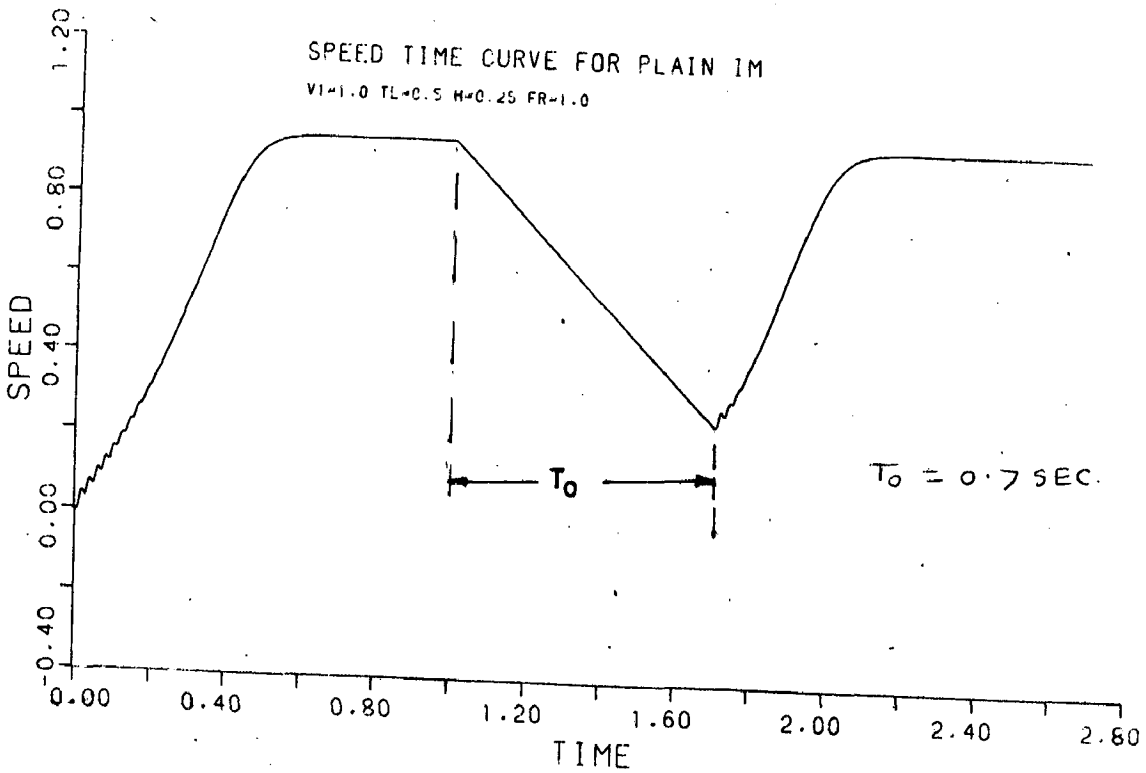
SPEED TIME CURVE FOR PLAIN IM
VI=1.0 TL=0.5 H=0.25 FR=1.0
SPEED
1.20
0.80
0.40
0.00
-0.40
T_0
T_0 = 0·7 SEC.
0.00
0.40
0.80
1.20
1.60
2.00
2.40
2.80
TIME

shows the transients when the motor starts from rest, attains steady state, gets disconnected from supply for a period of 0.1 sec and is reconnected to supply.

Fig. 4.2(d) shows similar transients when the reclosing has been delayed to 0.7 sec.

On the basis of these figures following points may be observed :

(i) The open circuit voltage falls to -0.424 p.u. after 0.1 sec. and 0.0 p.u. after 0.7 sec. and the corresponding resultant voltages are 1.424 p.u. and 1 p.u.respectively (Fig.4.2(a)).

(ii) The motor speed falls to 0.85 p.u.after 0.1 sec. and 0.3 p.u.after 0.7 sec. (Fig.4.2(b)).

(iii) The reclosing transients with 0.1 sec as reclosing time (Fig.4.2(c)) are much more severe than the one with 0.7 sec. as reclosure time (Fig.4.2(d)). It is due to the fact that initial momentary dynamic breaking torque due to assymmetrical flux is more in the case of 0.1 sec. The negative torque peak is clearly evident in Fig.4.2(c). Quantitative comparison shows that the peak torque in this case is - 3.3 p.u. as against + 2.7 p.u. for the case of Fig. 4.2(d). The settling time is, however more when reclosure time is more. In the present two cases it is 0.5 sec for the case of Fig.4.2(d) and 0.23 sec.for the case of Fig. 4.2(c).

(iv) The switching transients, obviously, remain same for the two cases of Fig.4.2(c)and (d).

These observations converge to the conclusion that reclosing torque transients are worst when reclosure occurs at an instant which corresponds to maximum resultant voltage at the motor terminals. In order to give further support to this conclusion, the peak reclosing torque transients have been obtained corresponding to several reclosure periods taken at regular interyals of 0.0025 sec. and its variation is plotted in Fig. 4.2(e). It clearly shows that the worst case is the one corresponding to a reclosing time of slightly greater than 0.1 sec. The peak torque for a reclosure time of 0.95 sec., when the motor speed falls to zero and its open circuit voltage has also vanished, is about 3.3 p.u. This must be same as the peak observed when the machine is started from rest. The switching transients of Figs. 4.2(c) and (d) provide this cross-check.

Having ascertained that the worst reclosure time for this induction motor operating under normal supply conditions with a constant load torque of 0.5 p.u., is slightly greate r than 0.1 sec, the effect of variations in supply voltage, supply frequency, inertia constant and load torque may now be discussed.

4.5.1.1 Effect of Variation in Supply Voltage

During operation of the machine it is likely that it may have to be operated for considerable period from ac supply whose voltage differs from normal value by ± 20%. The effect of reclosure under such abnormal operating conditions is investigated. Figs. 4.3(a) and (b) show the results.

(why?)

It is observed that if the supply interruption takes place when the motor was operating with 0.8 p.u. voltage, the worst instant of reclosure appears earlier than the normal case (1.0 p.u. voltage) and the resulting peak torque transient reduces in magnitude. The reverse happens when the applied voltage is more than normal value at the time of supply interruption. Table 4.1 shows the quantitative comparison.

It is also observed that in all the three cases, the worst reclosing instant appears slightly later than the instant when resultant voltage is maximum.

4.5.1.2 Effect of Variation in Supply Frequency

The effect of variation in supply frequency on reclosure is investigated. Figs. 4.4(a) and (b) show the results.

It is observed that if the supply interruption takes place when the motor was operating with 0.92 p.u. frequency, the worst instant of reclosure appears later than the normal

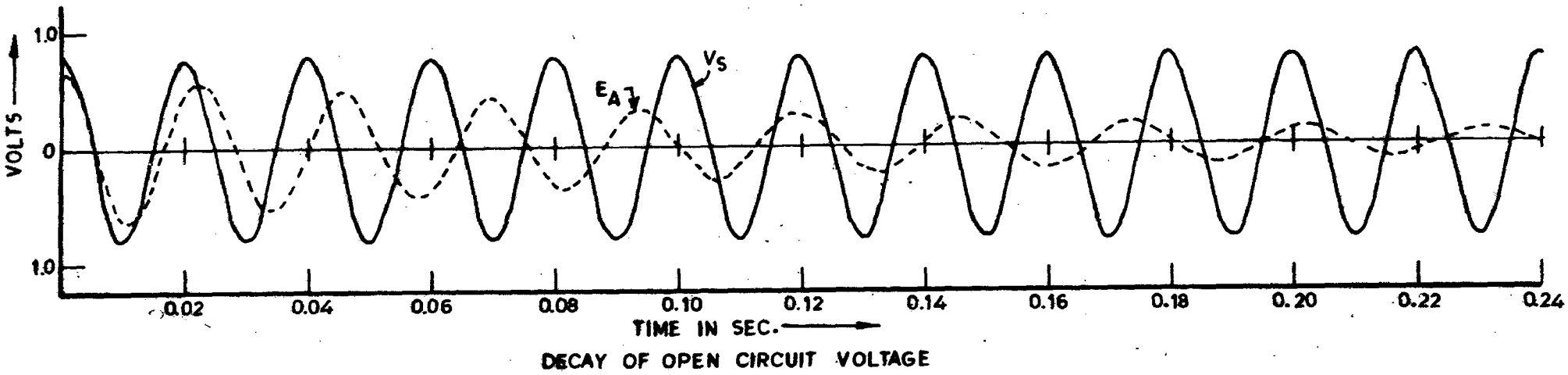

DECAY OF OPEN CIRCUIT VOLTAGE

1) MAXIMUM RESULTANT VOLTAGE OCCURS AFTER = T_{VRM} = 0.07 sec
2) WORST PEAK TORQUE OCCOURS WITH A RECLOSURE PERIOD ... ... = T_{WR} = 0.075 sec
3) WORST PEAK TORQUE ... ... = WPTE = 2.7 pu

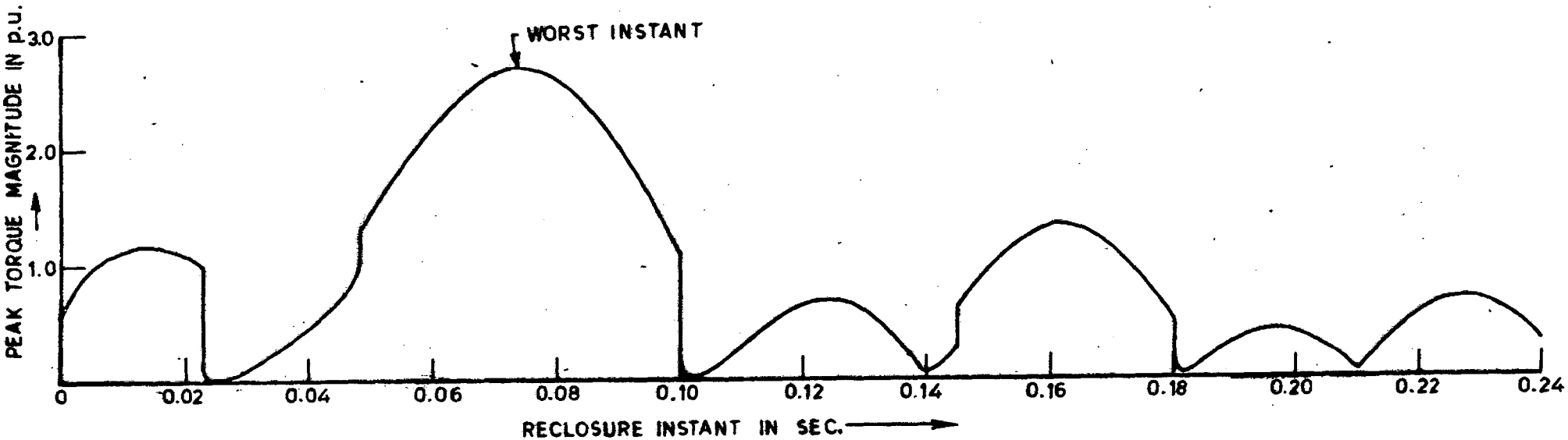

FIG. 4.3 (a) – PEAK RECORDING TORQUE VS RECLOSING TIME
[V_1 = 0.8 F_R = 1.0 H = 0.25 T_L = 0.5]

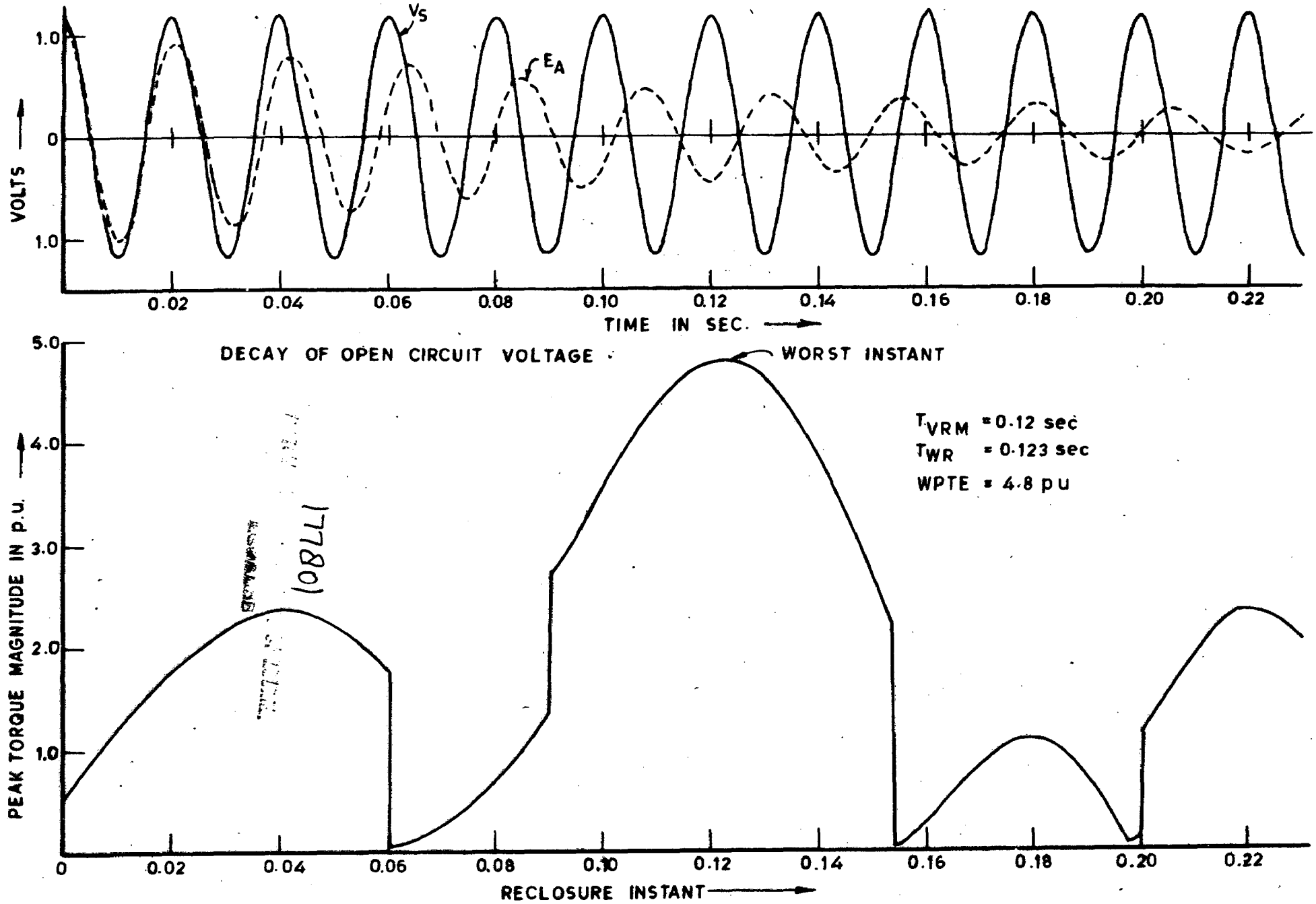

FIG. 4.3(b) _ PEAK RECLOSING TORQUE VS RECLOSING TIME
[$V_1 = 1.2$, $F_R = 1.0$, $H = 0.25$, $T_L = 0.5$]

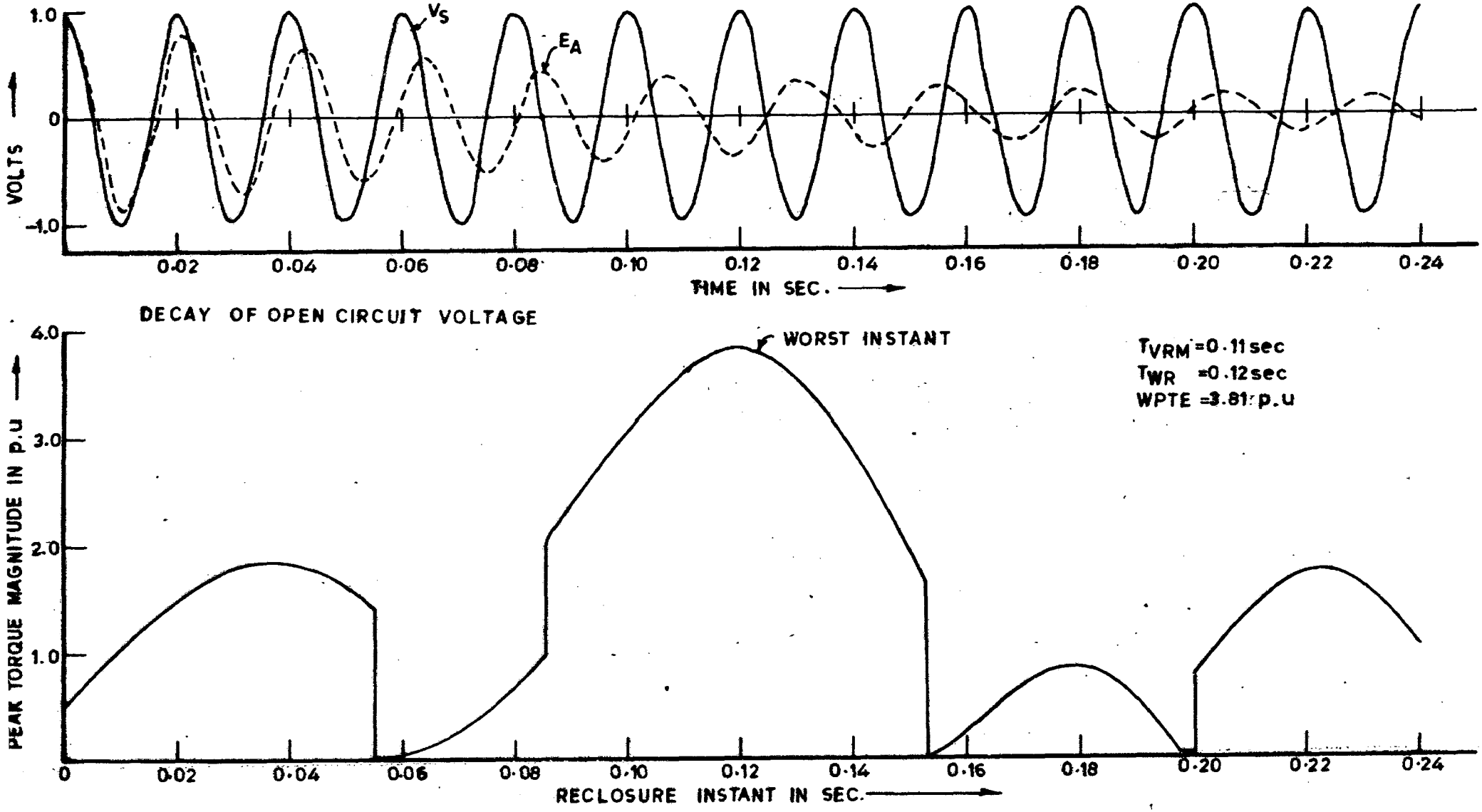

FIG. 4.4 (a) _ PEAK RECLOSING TORQUE VS RECLOSING TIME
[$V_1 = 1.0$, $F_R = 0.92$, $H = 0.25$, $T_L = 0.5$]

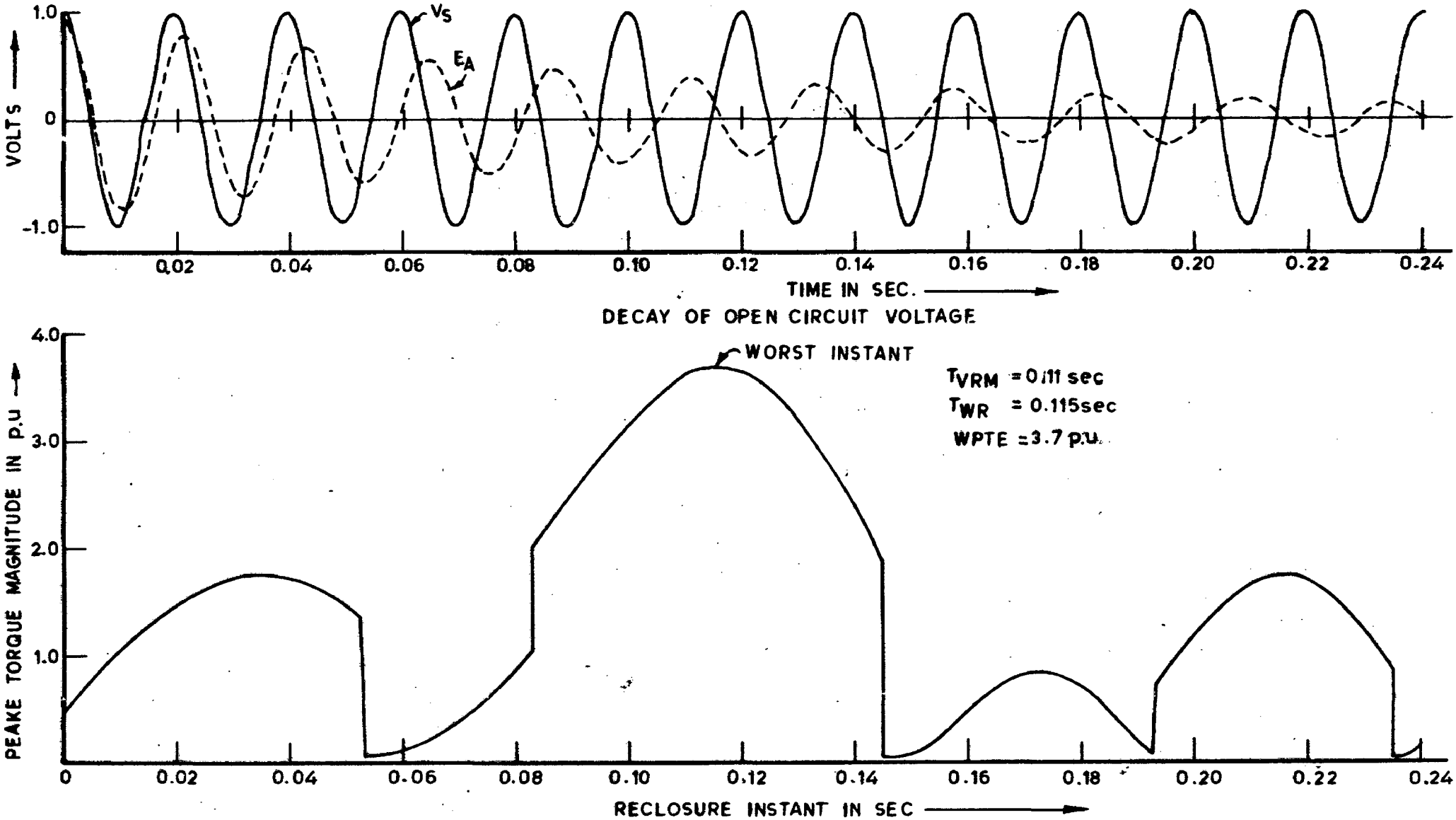

FIG. 4.4 (b) _ PEAK RECLOSING TORQUE VS RECLOSING TIME
[V_1 = 1.0, F_R = 0.96, H = 0.25, T_L = 0.5]

case (1.0 p.u. frequency) and the resulting peak torque transient increases in magnitude. The results are in the same line when motor is operating with 0.96 p.u. frequency.

Quantitative comparison is shown in Table 4.2.

It is observed that in all the three cases, the worst reclosing instant appears slightly later than the instant when resultant voltage is maximum.

4.5.1.3 Effect of Variation in Inertia Constant

There is a possibility that the inertia constant of the machine may change because of mounting or unmounting of certain components on the motor shaft. The effect of reclosure under such conditions is investigated. Figs. 4.5(a) show the results.

It is observed that if the supply interruption takes place with increased value of system inertia, the worst instant of reclosure appears later than the normal case (0.25 inertia) and the resulting peak torque transient increases slightly in magnitude. Table 4.3 shows the quantitative comparison.

It is observed as before, that the worst reclosing instant appears slightly later than the instant when resultant voltage is maximum.

4.5.1.4. Effect of Variation in Load Torque

The effect of variation in load torque on reclosure is investigated. Figs.4.6(a) and (b) show the results.